Tunable Optical Parametric Oscillators

STEPHEN E. HARRIS, MEMBER, IEEE

Invited Paper

Abstract—This paper reviews progress on tunable optical parametric oscillators. Topics considered include: parametric amplification of Gaussian beams; threshold; tuning techniques, spectral output, and stability; saturation and power output; spontaneous parametric emission; nonlinear materials; and far infrared generation.

Fig. 1. Schematic of optical parametric oscillator. The mirrors are highly reflecting at either the signal of idler, or both.

I. INTRODUCTION

WORK on optical parametric oscillators began in 1961 when Franken *et al.* [1] demonstrated second harmonic generation of light, and thus the existence of substantial nonlinear optical coefficients. Following a number of proposals and theoretical studies [2]–[6] Giordmaine and Miller, in 1965, constructed the first tunable optical parametric oscillator [7]. Since then, work has proceeded rapidly and it is now possible to tune through most of the visible and near infrared; to obtain greater than 50 percent conversion efficiency of the light from the laser pump; and to obtain linewidths of less than a wavenumber. With careful construction, threshold for a CW oscillator may be as low as 3 mW.

Many of the basic ideas of parametric amplification and oscillation have been extensively explored in the microwave frequency range [8]. If some upper frequency ω_p, termed as the pump, is incident on a material possessing a nonlinear reactance, then an incident signal frequency ω_s may be amplified. In the process a third frequency ω_i, termed as the idler frequency, and such that $\omega_s + \omega_i = \omega_p$ is generated. Irrespective of the phase of the incoming signal frequency, the phase of the idler may adjust such that the signal and idler are amplified, and the pump is depleted.

In the optical frequency range the nonlinear reactance is obtained via the nonlinear polarizability of noncentrosymmetric crystals [9]. This nonlinear polarizability is described by a 27 component tensor χ_{ijk} which relates the three components of the generated polarization $\mathscr{P}_i$ to the nine possible combinations of applied field $E_j E_k$. That is,

$$\mathscr{P}_i = \sum_j \sum_k \chi_{ijk} E_j E_k, \qquad (1)$$

where i, j, and k may be x, y, or z. Typically over the transparency range of the crystal, the nonlinear coefficients χ_{ijk}

are nearly independent of frequency, and, unlike the case for a laser transition, very wide tunability is possible.

Though in principle, the χ_{ijk} allow any three optical frequencies to interact, in order to achieve significant parametric amplification it is required that at each of the three frequencies (i.e., at the signal, idler, and pump) the generated polarization travel at the same velocity as a freely propagating electromagnetic wave. This will be the case if the refractive indices of the material are such that the k vectors satisfy the momentum matching condition $\bar{k}_s + \bar{k}_i = \bar{k}_p$ [10]. For collinearly propagating waves this may be written

$$\omega_s n_s + (\omega_p - \omega_s) n_i = \omega_p n_p, \qquad (2)$$

where n_s, n_i, and n_p are the refractive indices at the signal, idler, and pump. Once the pumping laser is chosen, and thus ω_p fixed, then if the refractive indices at the signal, idler, or pump frequencies are varied, the signal and idler frequencies will tune. Considerable control of the refractive indices, and very wide tuning, is possible by making use of the angular dependence of the birefringence of anisotropic crystals, and also by temperature variation. Rapid tuning over a limited range is possible by electro-optic variation of the refractive indices.

A schematic of a typical parametric oscillator is shown in Fig. 1. The oscillator consists of a nonlinear crystal and a pair of mirrors. As will be discussed later, the mirrors may be reflecting at either the signal or idler frequency, or at both frequencies. Ideally, 100 percent conversion of incident pump power to tunable signal and idler power is possible. The output of an optical parametric oscillator is very much like that of a laser. It is highly monochromatic with a spectrum consisting of one or a number of longitudinal modes. It is often a fundamental Gaussian transverse mode and may be highly collimated. To the eye, the output of a CW parametric oscillator exhibits the same sparkle effect as does a He-Ne gas laser.

One principal difference between a laser and an optical parametric oscillator is the ability of the former to collect and store wide-band uncollimated spectral energy. A laser's wavelength and linewidth are determined by the pertinent atomic transition and are not affected by the spectral or spacial distribution of the pumping radiation. However, in an optical parametric oscillator, phase coherence between

The author is with the Department of Electrical Engineering, Microwave Laboratory, Stanford University, Stanford, Calif. 94305.

TABLE I
REPRESENTATIVE PARAMETRIC OSCILLATOR EXPERIMENTS

Pumping Wavelength	Nonlinear Crystal	Tuning Range	Output Power	References
0.53 μ (doubled CaWO$_4$:Nd^{3+})	LiNbO$_3$	0.73 μ − 1.93 μ (temperature tuning)	10^3 W	[7], [23]
0.53 μ (doubled Nd^{3+} − Glass)	KDP LiNbO$_3$	0.96 μ − 1.18 μ 0.68 μ − 2.36 μ (angle tuning)	10^5 W 50 W	[97], [98] [25]
0.35 μ (tripled Nd^{3+} − Glass)	KDP	0.53 μ ± 10 percent 1.06 μ ± 10 percent (angle tuning)	~10^4 W	[98]
0.69 μ (ruby)	LiNbO$_3$	1.05 μ − 1.20 μ 1.64 μ − 2.05 μ (angle, temperature, and electrooptic tuning)	4 10^5 W	[29], [27], [34]
0.53 μ (doubled Nd^{3+}:YAG)	Ba$_2$NaNb$_5$O$_{15}$	0.98 μ − 1.16 μ (temperature tuning)	3 mW (CW)	[15]
0.5145 μ (argon)	LiNbO$_3$	0.68 μ − 0.71 μ 1.9 μ − 2.1 μ (temperature tuning)	3 mW (CW)	[19]
0.69 μ (ruby)	LiNbO$_3$	50 μ − 238 μ 0.696 μ − 0.704 μ (angle tuning)	~70 W 10^5 W	[88], [89]
1.06 μ (Nd^{3+}:YAG)	LiNbO$_3$	1.95 μ − 2.35 μ (temperature and angle tuning)	170 W peak 17 mW average (repetitively pulsed)	[42]

the signal, idler, and pump is very important; and either spectral or angular spread of the pump may increase its threshold or widen its linewidth.

Based on crystals presently being developed, it is likely that within a few years, narrow-band tunable sources will be available over the entire spectral region from 0.2 μ to greater than 100 μ. Like fixed frequency lasers, these sources should provide at least 10^6 times as much power per bandwidth per steradian as do traditional spectroscopic sources. Such sources are likely to have significant impact on many types of excited state spectroscopy, optical pumping, semiconductor studies, and photochemistry. Table I summarizes the characteristics of a number of parametric oscillator experiments which have been performed to date.

II. PARAMETRIC AMPLIFICATION

A. Amplification of Plane Waves

Consider waves with a pumping frequency ω_p and a signal frequency ω_s to be incident on a nonlinear material having a polarizability $\mathscr{P} \sim E^2$. Mixing of these waves generates a traveling polarization wave at the difference frequency ω_i. By adjusting the birefringence of the crystal, the polarization wave may be made to travel at the same velocity as a freely propagating idler wave, thus resulting in cumulative growth. The idler wave also mixes with the pump to produce a traveling polarization wave at the signal frequency, phased such that growth of the signal field also results. The process continues with the signal and idler fields both growing, and the pumping field decaying as a function of distance

in the crystal. The equations describing this process [8], [10]–[12], in MKS units, are

$$\frac{dE_s}{dz} = -j\eta_s\omega_s dE_p E_i^* \exp -j\Delta k z \qquad (3a)$$

$$\frac{dE_i}{dz} = -j\eta_i\omega_i dE_p E_s^* \exp -j\Delta k z \qquad (3b)$$

$$\frac{dE_p}{dz} = -j\eta_p\omega_p dE_s E_i \exp j\Delta k z, \qquad (3c)$$

where the quantities E_s, E_i, and E_p are the envelopes of the plane waves; e.g., $E_s(z, t) = \text{Re }[E_s \exp j(\omega_s t - k_s z)]$. The quantities η_s, η_i, and η_p are the plane wave impedances (377/refractive index) of the three waves, and d is the effective nonlinear coefficient. In general, d depends on the direction of propagation and on the polarization of the respective waves, and will be considered further in Section VII. We allow for a k vector mismatch

$$\Delta k = k_p - k_s - k_i. \qquad (4)$$

We first note that by taking the complex conjugate of (3a) and (3b) and multiplying (3a), (3b), and (3c) by $E_s/\eta_s\omega_s$, $E_i/\eta_i\omega_i$, and $E_p^*/\eta_p\omega_p$, respectively, [5] that

$$\frac{1}{\omega_s}\frac{d}{dz}\left(\frac{|E_s|^2}{2\eta_s}\right) = \frac{1}{\omega_i}\frac{d}{dz}\left(\frac{|E_i|^2}{2\eta_i}\right)$$
$$= -\frac{1}{\omega_p}\frac{d}{dz}\left(\frac{|E_p|^2}{2\eta_p}\right). \qquad (5)$$

Growth at the signal implies growth at the idler. Depending on the relative phases of the three frequencies, power may flow either from the lower frequencies to the upper frequency as is the case for second harmonic or sum frequency generation; or alternately from the pump to the lower frequencies as in difference frequency generation and parametric amplification.

If we neglect depletion of the pump, then (3a) and (3b) may be solved subject to the boundary conditions that $E_s = E_s(0)$ and $E_i = E_i(0)$ at $z = 0$. For a crystal length L, we obtain

$$E_s(L) = E_s(0) \exp\left(-j\frac{\Delta k L}{2}\right)\left[\cosh sL + j\frac{\Delta k}{2s}\sinh sL\right]$$
$$-j\frac{\kappa_s}{s}E_i^*(0)\exp\left(-j\frac{\Delta k L}{2}\right)[\sinh sL], \tag{6a}$$

and

$$E_i(L) = E_i(0) \exp\left(-j\frac{\Delta k L}{2}\right)\left[\cosh sL + j\frac{\Delta k}{2s}\sinh sL\right]$$
$$-j\frac{\kappa_i}{s}E_s^*(0)\exp\left(-j\frac{\Delta k L}{2}\right)[\sinh sL] \tag{6b}$$

where

$$\kappa_s = \eta_s\omega_s d E_p$$
$$\kappa_i = \eta_i\omega_i d E_p$$
$$\Gamma^2 = \kappa_s\kappa_i^* = \omega_s\omega_i\eta_s\eta_i|d|^2 E_p|^2$$

and

$$s = (\Gamma^2 - \Delta k^2/4)^{1/2}.$$

We first examine the single pass power gain when only a signal frequency is incident, i.e., take $E_i(0) = 0$. Defining $G = |E_s(L)/E_s(0)|^2 - 1$, we find from (6a)

$$G = \Gamma^2 L^2 \frac{\sinh^2\left(\Gamma^2 - \frac{\Delta k^2}{2}\right)^{1/2} L}{\left(\Gamma^2 - \frac{\Delta k^2}{4}\right)L^2}. \tag{7}$$

For a given crystal temperature and orientation, the center of the parametric gain linewidth occurs at that signal and idler frequency where $\Delta k = 0$. At line center the gain is thus $\sinh^2\Gamma L$, which for small gain is approximately $\Gamma^2 L^2$. Thus

$$G_{\text{small gain}} \cong \Gamma^2 L^2 = 2\omega_s\omega_i\eta_s\eta_i\eta_p|d|^2 L^2 P_p/A. \tag{8}$$

As an example, $\Gamma^2 L^2$ for a 1 cm crystal of $90°$ cut LiNbO$_3$ for $\lambda_s = \lambda_i = 1~\mu$ is approximately $0.1~P_p/A$, where P_p/A has units of MW/cm^2. From (8) it is seen that the gain of a nonlinear material is proportional to $|d|^2/n^3$, where n is the refractive index. This figure of merit, together with their transparency range, is shown for a number of nonlinear materials in Fig. 24. It is useful to note that when $\omega_s = \omega_i = \omega_p/2$ ($\omega_p/2$ is termed the degenerate frequency), that the single pass gain of an optical parametric amplifier is equal to the conversion efficiency (P_{SH}/P_F) of a second harmonic gen-
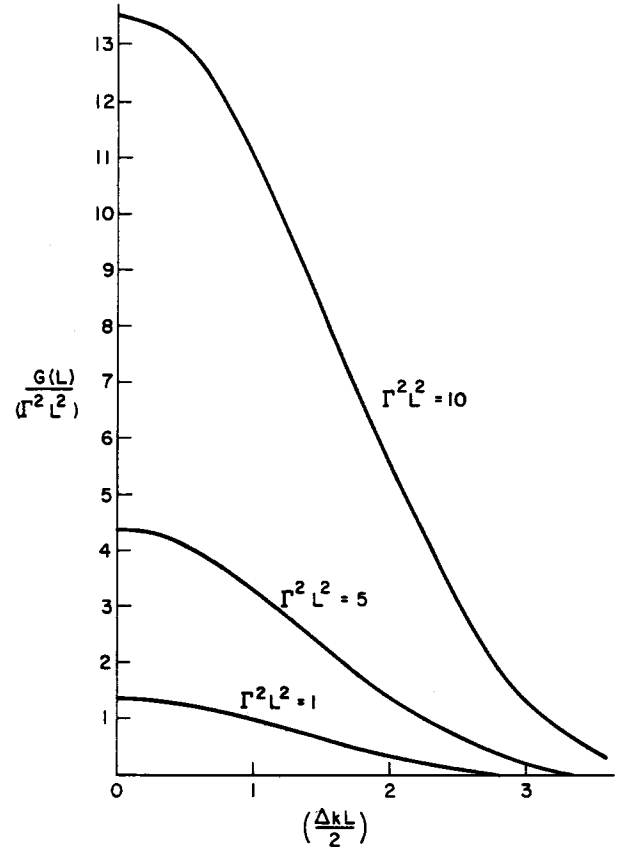

Fig. 2.   Normalized gain versus $(\Delta k L/2)$. (From Byer [96].)

erator with a fundamental frequency $\omega_p/2$. If we let $\omega_s = (\omega_p/2)(1 + \delta)$ and $\omega_i = (\omega_p/2)(1 - \delta)$, i.e.,

$$\delta = \frac{2\omega_s - \omega_p}{\omega_p} = \frac{2\lambda_p - \lambda_s}{\lambda_s}, \tag{9}$$

then the parametric gain off degeneracy is reduced from that on degeneracy by the factor $1 - \delta^2$.

The lineshape or dependence of the parametric gain on the optical frequency is determined by the variation of Δk with frequency. Noting that for $\Delta k^2 L^2/4 \gg \Gamma^2 L^2$ and small ΓL

$$G_{\text{small gain}} \cong \Gamma^2 L^2\left[\frac{\sin \Delta k L/2}{(\Delta k L/2)}\right]^2,$$

it is seen that for small gain, the full half-power gain linewidth is determined by $|\Delta k L| \cong 2\pi$. For a 4 cm crystal of LiNbO$_3$ at a pump wavelength of 4880 Å and a signal wavelength of 6328 Å, the dispersion is such that the half-power linewidth is about 1.4 cm^{-1} or about 0.56 Å. However, near degeneracy, linewidths may be much larger. From (7) it is seen that the gain linewidth is also somewhat dependent on $\Gamma^2 L^2$ and thus on the strength of the pump. Fig. 2 shows the quantity $G/\Gamma^2 L^2$ versus $(\Delta k/2)$.

B. Amplification of Gaussian Beams

In determining oscillator thresholds we will be concerned with the gain experienced by a fundamental Gaussian mode of the oscillator. In general, if a beam having a Gaussian

cross section is incident on a nonlinear crystal and parametrically amplified, the output beam will no longer be a simple Gaussian. This occurs as a result of Poynting vector walk-off (i.e., the fact that in an anisotropic crystal, the direction of power flow and $\bar{k}$ vector need not be the same); and also, in the absence of Poynting vector walk-off, as a result of the form of the nonlinear polarization generated in the parametric process.

The power gain experienced by an incident Gaussian mode may be found by evaluating an integral of the form $\int \bar{E}^* \cdot \bar{\mathscr{P}} dV$, where $\bar{E}$ is the electric field of the given mode, and $\bar{\mathscr{P}}$ is its driving polarization. A general analysis of this problem, allowing for arbitrarily tight focusing, and also for Poynting vector walk-off has been given by Boyd and Kleinman [13], and some of their results will be summarized in the latter part of this section. We first consider the more restricted but important case of near-field focusing and 90° phase matching (for 90° phase matching, Poynting vector walk-off is absent). An analysis of this case was first given by Boyd and Ashkin [14].

A near-field analysis keeps track of the transverse dependence of the signal, idler, and pump modes; but assumes that this transverse dependence does not change over the length of the nonlinear crystal. It thus requires that the confocal parameter of the focus (of all three beams) be as long or longer than the length of the nonlinear crystal.

To make the appropriate modification of the previous analysis we allow the signal, idler, and pump fields to have Gaussian cross-sectional dependencies of the form $E_{s0} \exp -r^2/W_s^2$, $E_{i0} \exp -r^2/W_i^2$, and $E_{p0} \exp -r^2/W_p^2$, respectively. The generated driving polarizations at the signal, idler, and pump are then also Gaussians [14] having beam waist radii $\bar{W}_s$, $\bar{W}_i$, and $\bar{W}_p$ given by

$$\frac{1}{\bar{W}_s^2} = \frac{1}{W_i^2} + \frac{1}{W_p^2} \tag{10a}$$

$$\frac{1}{\bar{W}_i^2} = \frac{1}{W_s^2} + \frac{1}{W_p^2} \tag{10b}$$

$$\frac{1}{\bar{W}_p^2} = \frac{1}{W_s^2} + \frac{1}{W_i^2}. \tag{10c}$$

For instance, the idler and pump mix to yield a polarization at the signal frequency of the form

$$\exp -\frac{r^2}{\bar{W}_s^2} = \exp -\frac{r^2}{W_i^2} \exp -\frac{r^2}{W_p^2}.$$

Note that these polarization radii are always smaller than the radius of either of the Gaussian beams which mix to produce them. We take the appropriate projections of these Gaussian polarizations by multiplying them by $\exp -r^2/W_s^2$, $\exp -r^2/W_i^2$, and $\exp -r^2/W_p^2$, respectively, and integrating over the transverse cross sections. The result of this is the set of equations

$$\frac{dE_{s0}}{dz} = -j\eta_s \omega_s d g_s E_{p0} E_{i0}^* \exp -j\Delta k z \tag{11a}$$

$$\frac{dE_{i0}}{dz} = -j\eta_i \omega_i d g_i E_{p0} E_{s0}^* \exp -j\Delta k z \tag{11b}$$

$$\frac{dE_{p0}}{dz} = -j\eta_p \omega_p d g_p E_{s0} E_{i0} \exp j\Delta k z, \tag{11c}$$

where the spatial coupling factors g_s, g_i, and g_p are

$$g_s = 2\frac{\bar{W}_s^2}{W_s^2 + \bar{W}_s^2}; \quad g_i = 2\frac{\bar{W}_i^2}{W_i^2 + \bar{W}_i^2}; \quad g_p = 2\frac{\bar{W}_p^2}{W_p^2 + \bar{W}_p^2}. \tag{12}$$

These coupling factors are a measure of the failure of the driving polarizations to completely overlap the desired Gaussian modes. If (though this can never be the case) $\bar{W}_s = W_s$, $\bar{W}_i = W_i$, and $\bar{W}_p = W_p$, then $g_s = g_i = g_p = 1$. Except for these coupling factors, (11) is identical to (5); and the solutions of the previous section may be employed.

The parametric gain coefficient Γ^2 of (8) thus becomes

$$\underset{\text{Gaussian beams}}{\Gamma^2 L^2} = \omega_s \omega_i \eta_s \eta_i |d|^2 g_s g_i L^2 |E_{p0}|^2, \tag{13}$$

where, from (10) and (12) the factor $g_s g_i$ is

$$g_s g_i = 4 W_p^2 \left[\frac{W_s W_i W_p}{W_s^2 W_i^2 + W_s^2 W_p^2 + W_i^2 W_p^2} \right]^2. \tag{14}$$

The power of the Gaussian pump beam is given by $(E_{p0}^2/2\eta_p)(\pi W_p^2/2)$, and thus (13) may be rewritten

$$\Gamma^2 L^2 = \frac{16}{\pi} \omega_s \omega_i \eta_s \eta_p \eta_i |d|^2 L^2 P_p M^2, \tag{15}$$

where

$$M^2 = \left[\frac{W_s W_i W_p}{W_s^2 W_i^2 + W_s^2 W_p^2 + W_i^2 W_p^2} \right]^2,$$

and P_p is the incident pump power.

Ashkin and Boyd [14] have shown that to maximize M^2 for W_s and W_i fixed, that the pumping beam size W_p^2 should be

$$\frac{1}{W_p^2} = \frac{1}{W_s^2} + \frac{1}{W_i^2}, \tag{16a}$$

in which case M^2 will be

$$M_{\max}^2 = \frac{1}{4} \frac{1}{W_s^2 + W_i^2}. \tag{16b}$$

In order to maximize the parametric gain at a given pump power, W_s and W_i should be chosen as small as possible. However, since the present analysis is restricted to the near field, the smallest allowed spot sizes are approximately those of the confocal condition, i.e., $W_s^2 = L\lambda_s/2\pi n_s$, $W_i^2 = L\lambda_i/2\pi n_i$. From (16a), if both the signal and idler are confocally focused, it is seen that the pump should also be confocally focused [14].

Combining the previous equations, and making use of the degeneracy factor of (9), the single pass parametric gain coefficient $G = \Gamma^2 L^2$ for a confocally focused signal, idler, and pump may be written

$$\Gamma^2 L^2 = 2\omega_0^2 \eta^3 |d|^2 L^2 \frac{P_p}{\pi W_0^2} (1 - \delta^2)^2, \tag{17}$$

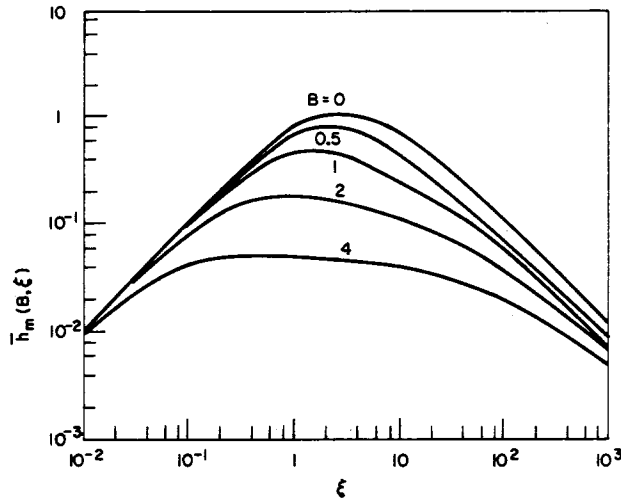where ω_0 is the degenerate frequency and $W_0^2 = (L\lambda_0)/(2\pi n)$

Fig. 3. Reduction factor $\bar{h}_m(B, \xi)$ versus ξ.
(From Boyd and Kleinman [13].)

TABLE II
REPRESENTATIVE 90° PHASE MATCHABLE MATERIALS

Material	λ_p	Crystal length	P_p/A for 30 percent gain	P_p for 30 percent gain (confocal focusing)	Linewidth
ADP	2573 Å	5.0 cm	0.76 MW/cm²	39 watts	8 cm⁻¹
LiNbO₃	5300 Å	4.0 cm	0.18 MW/cm²	15 watts	1 cm⁻¹
Ba₂NaNb₅O₁₅	5300 Å	0.5 cm	1.6 MW/cm²	17 watts	8 cm⁻¹
CdSe	2.5 μ	2.0 cm	0.77 MW/cm²	141 watts	~15 cm⁻¹

is the degenerate confocal spot size. The price for moving off degeneracy is the factor $(1 - \delta^2)^2$. For example, if $\lambda_p = 0.473 \ \mu$ and $\lambda_s = 0.54 \ \mu$, then $\delta = 0.75$ and $(1 - \delta^2)^2 = 0.188$; and the threshold is about five times higher than if $\lambda_s = \lambda_i \doteq 2\lambda_p$. Substituting for W_0, (17) becomes

$$\Gamma^2 L^2 = \frac{16\pi^2 d^2 L}{c e_0^3 n^2 \lambda^3} P_p (1 - \delta^2)^2. \tag{18}$$

For a crystal of LiNbO₃ at a degenerate wavelength of 1 μ, this yields

$$\Gamma^2 L^2 \cong 0.005 \ L P_p (1 - \delta^2)^2, \tag{19}$$

where L is in cm, and P_p in watts. Note that for optimum focusing $\Gamma^2 L^2$ increases only linearly with crystal length. Thus 1 watt of pumping power in a 4 cm LiNbO₃ crystal provides 2.0 percent single pass gain at a degenerate wavelength of 1 μ.

We now proceed with some of the results of the Boyd and Kleinman analysis [13]. Allowing for both Poynting vector walk-off and arbitrarily tight focusing they show that the effective single pass gain of interacting Gaussian modes all having the same confocal parameter is given by (18) multiplied by a reduction factor $\bar{h}_m(B, \xi)$. The parameter ξ is the ratio of the length of the nonlinear crystal to the common confocal parameter b_0; and B is a double refraction parameter [13] defined as

$$B = \frac{\rho}{2} \left(\frac{2\pi L n_0}{\lambda_0} \right)^{1/2} \left(\frac{n_3}{n_0} \right)^{1/2}, \tag{20}$$

where ρ is the walk-off angle, L is the length of the nonlinear crystal, λ_0 is the degenerate wavelength, and n_0 and n_3 are the refractive indices at the degenerate wavelength and pump, respectively. B is approximately the ratio of the walk-off angle ρ to the far field diffraction angle of the Gaussian beam.

The reduction factor $\bar{h}_m(B, \xi)$ as a function of ξ with B as a parameter is shown in Fig. 3. In the absence of double refraction (90° phase matching), $B = 0$, and for optimum focus-

ing $\xi = L/b_0$ should be 2.84. However, the increase in gain over that obtained for $L/b_0 = 1$, used in the previous near-field analysis, is only about 20 percent and may not be worth the increased pump power density at the tighter focus. It should also be mentioned that at the tighter focusing, Δk should be slightly different from zero. This results since, at a tight focus, the mixing of the noncollinear components of the signal and idler fields requires slightly longer $\bar{k}$ vectors than does the collinear mixing. This optimized $\bar{k}$ vector match [13] is included in the function $\bar{h}(B, \xi)$.

In many practical cases B will be sufficiently large so that, as seen in Fig. 3, the maximum value of $\bar{h}_m(B, \xi)$ will be rather independent of ξ. Boyd and Kleinman [13] have shown that for large B,

$$\bar{h}_m(B, \xi) \to \pi/4B^2 \qquad (B^2/4 > \xi > 2/B^2), \tag{21}$$

where for the range of B and ξ shown in parenthesis, (21) is correct to within 10 percent. Since B^2 is proportional to L, the L in the numerator of (18) is cancelled, and for large birefringence the gain is nearly independent of the length of the nonlinear crystal; and subject to the criteria of (21), to the degree of focusing. Since for 90° phase matching $\bar{h}_m(B, \xi) \cong 1$, the factor $\pi/4B^2$ is approximately the gain reduction factor which is experienced as a result of walk-off.

As an example, to phase match a LiNbO₃ parametric oscillator directly pumped by a 1.06 μ Nd³⁺:YAG laser at 90° requires a crystal temperature of about 750°C [13]. Room temperature phase matching at degeneracy is accomplished by propagating at an angle of 43° with respect to the optic axis. This yields a walk-off angle $\rho = 0.037$ radians and $B \cong 4.7 \ L^{1/2}$. For a 1 cm crystal the maximum gain at a given pump power is then 28 times smaller than it would have been had 90° phase matching been possible.

It should be noted that the above discussion is concerned with gain maximization at a given pump power as opposed to at a given pump power density. If maximization is with regard to power density, walk-off need not be of consequence. If the beam radii of all modes are greater than $W_0 = \sqrt{2\rho L}$, then the gain reduction due to walk-off will be less than 15 percent and may be made essentially negligible for still bigger beams [14].

Table II shows the approximate pump power densities and optimized pump powers necessary to obtain 30 percent single pass gain with typically available lengths of some nonlinear crystals. Approximate gain linewidths for these crystal lengths are also shown.

III. THRESHOLD PUMPING POWER

To construct an oscillator it is necessary to resonate either the signal or the idler, or both. The latter case, where both the signal and idler are resonant, yields the lowest threshold, but poses severe stability problems and mirror requirements. Since they have the lowest threshold, oscillators of this type have thus far been the most prevalent.

To determine threshold of the oscillator we require that the single pass parametric gain (note that there is only gain when the signal and idler travel in the direction of the pump) be sufficient to offset the round-trip cavity loss. We define α_s and α_i as the round-trip $\bar{E}$ field losses at the signal and idler frequencies, e.g., $E_s(0) = (1 - \alpha_s)E_s(L)$. From (6) for $\Delta k = 0$, we require

$$\frac{1}{1 - \alpha_s} E_{s0}(0) = E_{s0}(0) \cosh \Gamma L - j\frac{\kappa_s}{s} E_{i0}^*(0) \sinh \Gamma L \quad (22a)$$

$$\frac{1}{1 - \alpha_i} E_{i0}(0) = E_{i0}(0) \cosh \Gamma L - j\frac{\kappa_i}{s} E_{s0}^*(0) \sinh \Gamma L, \quad (22b)$$

where E_{s0} and E_{i0} are the peak amplitudes of the Gaussian modes as defined in the previous section; Γ is defined by (13); and κ_s and κ_i are given by $\eta_s \omega_s dE_p g_s$ and $\eta_i \omega_i dE_p g_i$, respectively. Taking the complex conjugate of (22b) and setting the determinant of the resulting two simultaneous equations equal to zero, we obtain

$$\left(\cosh \Gamma L - \frac{1}{1 - \alpha_s}\right)\left(\cosh \Gamma L - \frac{1}{1 - \alpha_i}\right) - \sinh^2 \Gamma L = 0$$

$$\cosh \Gamma L = 1 + \frac{\alpha_s \alpha_i}{2 - \alpha_s - \alpha_i}. \quad (23)$$

For low loss resonators at both the signal and idler frequencies, (23) is satisfied by

$$\Gamma^2 L^2 \cong \alpha_s \alpha_i. \quad (24)$$

signal and idler resonant
small losses

Alternately, if only the signal is resonant and it is assumed that no idler radiation is returned to the crystal input ($\alpha_i = 1$) than for small α_s

$$\Gamma^2 L^2 = 2\alpha_s. \quad (25)$$

signal only resonant
small losses

The ratio of threshold pump power with the signal only resonant as compared to both signal and idler resonant is $2/\alpha_i$. Thus for a 2 percent idler cavity loss, one-hundred times as much power is required for the signal-only-resonant case. It should be noted that for small losses the round-trip $\bar{E}$ field losses α_s and α_i are also the single pass power losses at the respective frequencies.

From (24) and (25) it is seen that parametric gains which are far too small to be useful for tunable amplification are sufficient to attain threshold in a parametric oscillator [14]. For single pass signal and idler power losses of 2 percent each, (24) yields $\Gamma^2 L^2 = 4 \times 10^{-4}$. Equation (19) shows that to attain this gain in a 4 cm crystal of LiNbO₃ at a degenerate wavelength of 1 μ requires a pump power of only
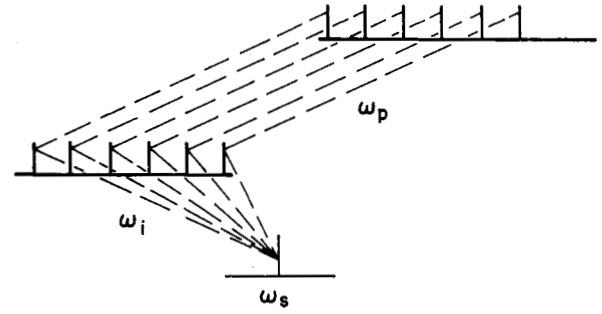

Fig. 4. Pumping with a multimode pump.

20 mW. The possibility of CW parametric oscillators with such low thresholds was first pointed out by Boyd and Ashkin [14], and first demonstrated by Smith et al. [15]. Their first oscillator employed a 5 mm crystal of $Ba_2NaNb_5O_{15}$ and was pumped by a doubled 1.06 μ Nd^{3+}:YAG laser. Threshold was observed at 45 mW of multimode power. More recently, Smith [16] has constructed a CW argon pumped oscillator with a threshold of about 2 mW.

The formulas of this section have implied that the pumping radiation consists of only a single longitudinal mode. For a parametric oscillator with both its signal and idler cavities resonant, Harris has shown [17] that if the axial mode interval of the idler frequency is set equal to that of the pumping laser, then all of the modes of the pumping laser may act in unison to produce gain at a single signal frequency mode. Though the pump modes are randomly phased, the idler modes develop compensating phases which maximize the gain of the system [18]. A schematic of this idea is shown in Fig. 4. Using it, Byer et al. [19] demonstrated an argon pumped visible CW oscillator with a tuning range of 0.68 μ–.71 μ in the visible and corresponding 1.9 μ–2.1 μ range in the IR. The oscillator used a 1.65 cm long crystal of LiNbO₃ and had a threshold of about 500 mW.

It has also been shown that if the dispersion of the nonlinear crystal is sufficiently small that the axial mode interval of both the signal and idler may be set equal to that of the pump, then the peak power, as opposed to the average power of the pump drives the oscillator [20]. The pump could then be phase locked and threshold obtained at a lower average power.

For the case of the signal-only resonant oscillator, the idler modes are not constrained, and thus though it has not been formally proven, the full average power of a multimode laser should be useful. Further, if the axial mode interval of the signal frequency is set equal to that of the pump, then peak power should be the pertinent quantity.

It should perhaps be mentioned that for many parametric oscillators pumped with Q-switched lasers, the problem is not one of attaining threshold, but of having sufficient gain for a sufficient time for the oscillation to build out of the noise. To deplete the pump requires about 140 dB of total gain. If we assume that the round-trip transit time of the oscillator is 1 ns, and if the length of the Q-switched pulse of the pumping laser is 20 ns; then the apparent threshold
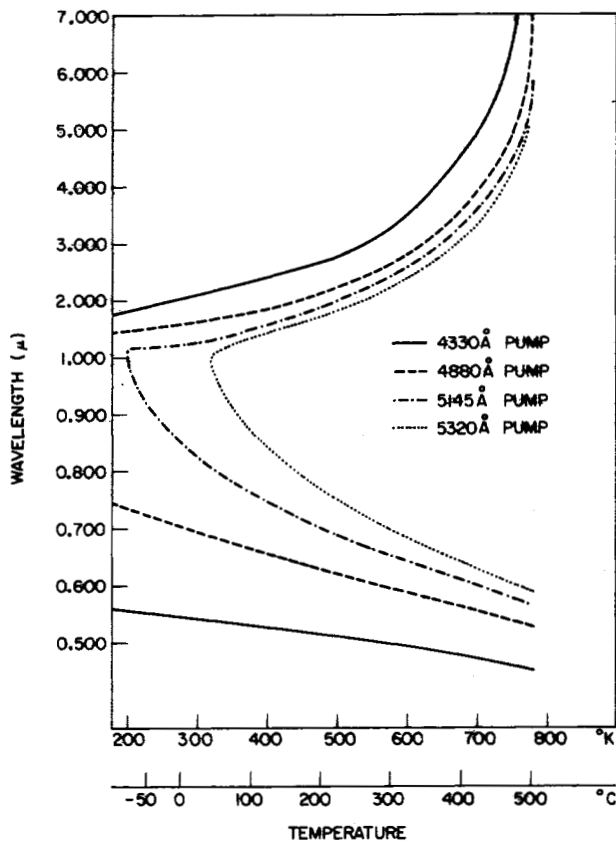
Fig. 5.   Temperature tuning of LiNbO₃ for several pump wavelengths. Data were obtained from the Sellmeier equations and [21]. (From Byer [96].)
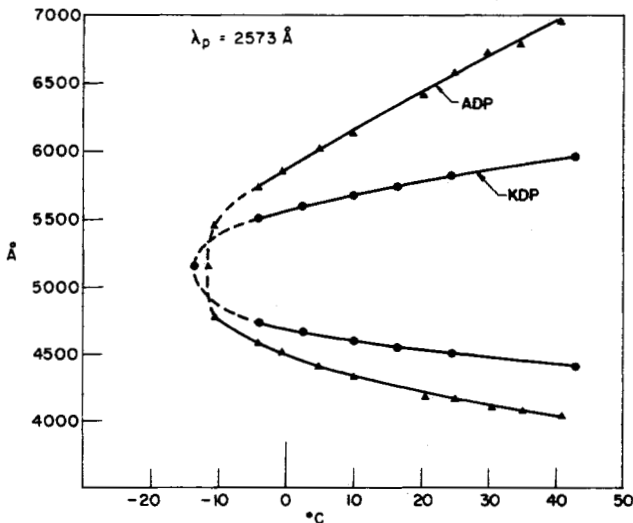

Fig. 6.   Temperature tuning of ADP and KDP. These curves were obtained by Dowley [24] using the spontaneous parametric emission technique discussed in Section VI.
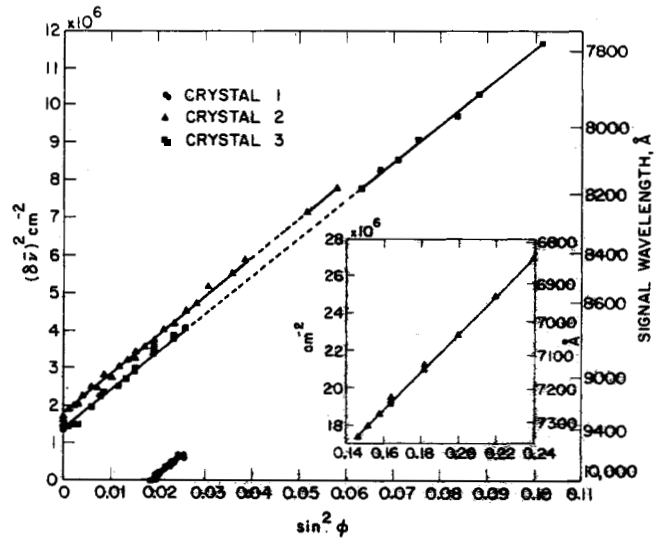

Fig. 7.   Angular tuning of LiNbO₃ oscillator. The angle ϕ is the complement of the internal angle between the optic axis and the direction of propagation of the pump. The shift in wavenumbers from the degenerate frequency $\bar{\nu} = 9434$ cm is denoted by $\delta\bar{\nu}$. Data connected by solid lines were obtained with a single pair of mirrors. (From Miller and Nordland [25].)
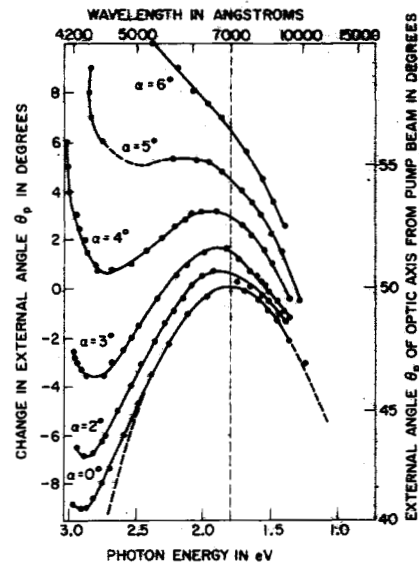

Fig. 8.   Angular tuning of ADP at 3472 Å. α is the angle between the pumping beam and the direction of observation of spontaneously emitted light. Thus, $\alpha = 0°$ gives the tuning curve of a collinear oscillator. The right-hand ordinate gives the approximate angle θ_p between the optic axis and pump direction. (Magde and Mahr [46].)
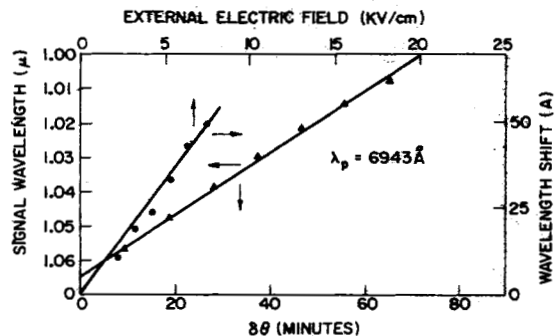

Fig. 9.   Electrooptic tuning. Wavelength shift as a function of the external dc electric field; and oscillator signal wavelength as a function of $\delta\theta$, the change in angle between $\bar{k}_p$ and the crystal optic axis. (Kreuzer [27].)

of the oscillator will be a pumping power which yields somewhat less than about 7 dB gain per pass.

IV. TUNING, SPECTRAL OUTPUT, AND STABILITY

A. Tuning

As noted earlier, the position of the center of the parametric gain linewidth is determined by satisfaction of the $\bar{k}$ vector matching condition $\bar{k}_s + \bar{k}_i = \bar{k}_p$, and the frequency condition $\omega_s + \omega_i = \omega_p$. For collinearly propagating forward waves these are combined to yield (2). With the pump frequency fixed, any process which changes the refractive indices at the signal, idler, or pump wavelengths will tune the oscillator. Tuning methods include: temperature, angular variation of the extraordinary refractive index, electro-optic variation of the refractive indices, and, perhaps, pressure tuning via the photoelastic effect. Of these, temperature or angular tuning may be used to tune over broad ranges, and pressure or electric fields may be used for fine tuning.

Temperature tuning curves for $LiNbO_3$ for a number of different pump wavelengths are shown in Fig. 5. The curves were obtained numerically from the Sellmeier equations of Hobden and Warner [21]. They may be shifted by 30° to 100° by changes in crystal composition [22]. Giordmaine and Miller [23] have experimentally temperature tuned a $LiNbO_3$ oscillator over the range 7300 Å – 19 300 Å.

Fig. 6 shows the temperature tuning curves for ADP and KDP pumped with the doubled 5145 Å line of argon. These curves were obtained experimentally by Dowley [24] by means of the parametric spontaneous emission method which will be discussed in Section VI. Note that the full visible spectrum is tuned by a variation of only 50°C.

Angular tuning curves for a $LiNbO_3$ parametric oscillator pumped by doubled 1.06 μ [25], and for an ADP oscillator pumped by doubled ruby, are shown in Figs. 7 and 8 [26]. The first of these was obtained in an oscillator experiment, and the second was obtained via spontaneous parametric emission. The angle ϕ in Fig. 7 is the complement of the internal angle between the optic axis and the direction of propagation of the pump, i.e., $\phi = 0$ for 90° phase matching. For the ADP oscillator a change of about 8° of the angle between the optic axis and pump beam tunes most of the visible spectrum. Though the angular tuning method is mechanical and potentially fast compared to temperature tuning, its disadvantage is the reduced gain which results from Poynting vector walk-off (Section II-B).

Experimental results of electrooptic tuning are shown in Fig. 9 [27]. The oscillator was $LiNbO_3$ pumped by ruby and had a tuning rate of about 6.7 Å per kV per cm of applied electric field. The angular tuning rate of this oscillator is also shown. Electrooptic tuning has also been demonstrated by Krivoshchekov et al. [28].

Another tuning technique is shown schematically in Fig. 10 [29]. In this case, the $\bar{k}$ vector matching is not collinear [30] and the oscillator is tuned by varying the angle between the incoming pump beam and the signal cavity. This type of tuning has the advantage that the nonlinear crystal need not be rotated inside the optical cavity. Instead either the angle of the input pump is varied via a beam deflector or alter-
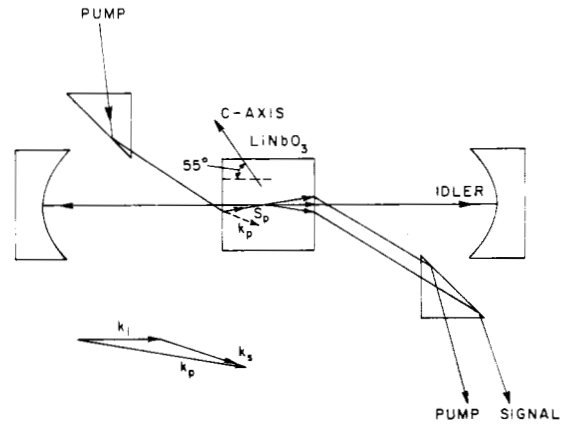

Fig. 10. Schematic of noncollinear oscillator. Tuning is accomplished by varying the angle between the pump and signal cavity. (From Falk and Murray [29].)
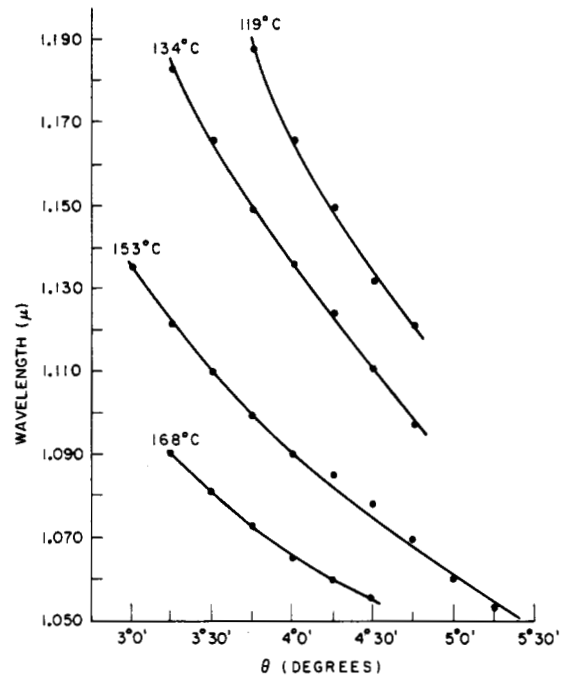

Fig. 11. Tuning of the noncollinear oscillator at different temperatures. (From Falk and Murray [29].)

nately, as was done in the experiment of Fig. 10, the entire cavity containing the nonlinear crystal is rotated. Results of this experiment are shown in Fig. 11 [29].

If we let ζ denote any variable which may be used to vary the refractive indices, and if we assume the pump frequency fixed, then for collinear phase matching the rate of signal frequency tuning with ζ is given by

$$\frac{d\omega_s}{d\zeta} = \frac{1}{b}\left[\frac{\partial k_p}{\partial \zeta} - \frac{\partial k_s}{\partial \zeta} - \frac{\partial k_i}{\partial \zeta}\right], \qquad (26)$$

where b is a dispersive constant [31] given by

$$b = \frac{\partial k_i}{\partial \omega_i} - \frac{\partial k_s}{\partial \omega_s}. \qquad (27)$$

In Section II-A, the half-power gain linewidth was shown to be determined approximately by the condition $|\Delta k L| = 2\pi$. Noting that $\Delta \omega_i = -\Delta \omega_s$, then from (4), $\Delta k = b\Delta \omega_s$. Thus the full half-power gain linewidth in Hz is
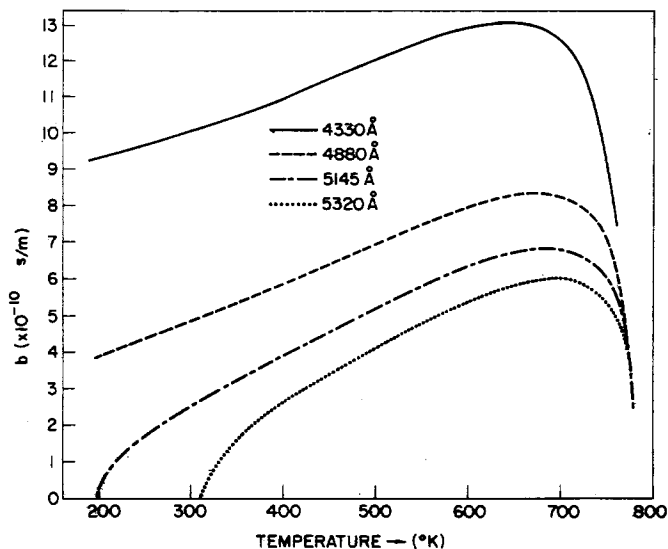
Fig. 12. Dispersion constant b versus temperature for LiNbO$_3$ at a number of pump wavelengths. Data were obtained from the Sellmeier equations of Hobden and Warner [21]. (From Byer [96].)

$$|\Delta f| \cong \frac{1}{bL}. \tag{28}$$

From (26) and (28) it is seen that materials with small b in general have large tuning rates, but also correspondingly large linewidths. Also, near degeneracy where the linewidth of an oscillator is large, it will, in general, tune much more rapidly than when far from degeneracy. As an example, KDP has a b that is about $\frac{1}{8}$ that of LiNbO$_3$, and as a result tunes much more rapidly (see Fig. 5 and 6). On the other hand, the linewidth of a 1 cm crystal of KDP is about 40 cm^{-1}, as compared to about 5 cm^{-1} for LiNbO$_3$.

The rate of change of the center of the parametric linewidth with respect to fluctuation of the pump frequency has been examined by Kovrigin and Byer [32].

B. Spectral Properties

The spectral character of the output of an oscillator is determined by the width and saturating behavior of the gain lineshape, and by the interaction of its signal and idler modes. Even for materials with relatively large b the half-power gain width will typically be greater than 1 cm^{-1} (30 GHz); and a number of axial modes at the signal and idler frequencies will lie within the linewidth. For instance for a 4 cm crystal of LiNbO$_3$ with a pump at 4880 Å and a signal at 6328 Å, $b=6.2 \times 10^{-10}$ s/m yielding a half-power width of 1.34 cm^{-1}. With mirrors placed on the ends of the crystal the axial mode spacing would be about 1.6 GHz and about 25 signal and idler modes would experience significant gain. Near degeneracy, typical observed linewidths are greater than 100 cm^{-1}. Fig. 12 shows the dispersive constant b for LiNbO$_3$ versus temperature at a number of pump wavelengths. Corresponding signal and idler frequencies as a function of temperature are shown in Fig. 5.

Parametric oscillators with both their signal and idler frequencies resonant pose a particularly severe problem [7], [11]. Since, as a result of dispersion, the axial mode spacing of the signal and idler frequencies are slightly different, simultaneous resonance of a signal and an idler
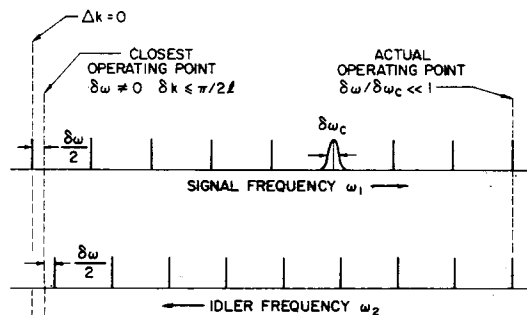

Fig. 13. Longitudinal modes of signal and idler cavities. Frequencies ω_1 and ω_2 vertically in line on the diagram satisfy $\omega_1 + \omega_2 = \omega_3$. The vertical dashed line farthest to the left indicates the frequency combination for index matching. The adjacent line represents the nearest frequency combination for which oscillation is possible. Since the frequency offset $\delta\omega$ is comparable to the cavity linewidth $\Delta\omega_c$, oscillation actually occurs at the vertical dashed line at the right where $\delta\omega = 0$. (From Giordmaine and Miller [11].)
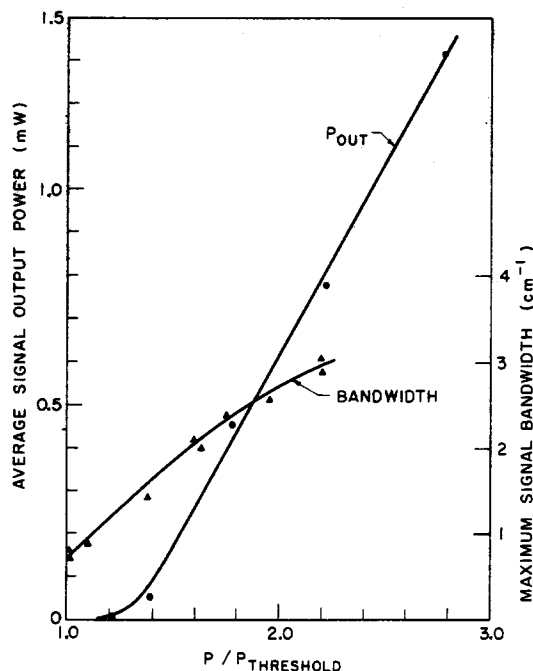

Fig. 14. Power output and linewidth versus P_p/P_p (threshold) of a CW argon pumped LiNbO$_3$ oscillator. (From Byer et al. [19].)

mode whose sum frequency is equal to the frequency of a pump mode, can only occur for certain axial modes. As shown in Fig. 13 the particular modes which happen to align may be far from the center of the gain linewidth. Furthermore, as a result of temperature changes and vibration, the modes which happen to align typically change very rapidly. This is particularly true when combined with the fact that the pump frequency is itself usually fluctuating [15]. For oscillators thus far constructed this fluctuation has had a time constant between about 10 μs and 1 ms, and has often severely reduced their average power output. Since the modes which align or nearly align are typically clustered together in groups having a spacing which is large compared to the axial mode spacing, this effect has been termed a "cluster effect" [7], [11].

The right scale of Fig. 14 shows the total spectral width of a 5145 Å argon pumped CW oscillator [19]. The data were
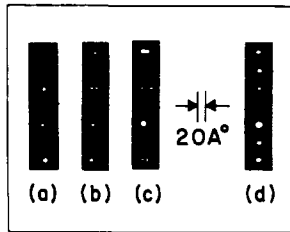
Fig. 15. Spectra of doubly and singly resonant oscillators. (a), (b), and (c) Spectra of the doubly resonant oscillator for increasing pump power. (d) Spectra of a singly resonant oscillator. (From Bjorkholm [34].)

Fig. 16. Schematic of frequency locking technique. The letters s, i, and p denote the signal, idler, and pump. respectively. The gas transition is assumed to absorb at only the signal frequency; and the mirrors are assumed to have high reflectivity at only the idler frequency. The vertical arrows in the LiNbO$_3$ crystals denote the direction of their positive z axes. (From Harris [37].)

obtained by taking a long-term exposure with a scanning Fabry–Perot etalon. With the oscillator operated about two times above threshold, the spectral width approaches the theoretical 4 wavenumber linewidth of the 1.65 cm LiNbO$_3$ crystal. For weaker pump drives, only modes closer to $\Delta k = 0$ were above threshold, and the spectral width is reduced. Average signal power output is also shown.

The cluster problem may be eliminated by constructing the oscillator with only its signal or its idler cavity, but not both, resonant. Feedback at the nonresonated frequency can be prevented by careful choice of mirrors, by the use of an appropriate absorbing material in the oscillator, or by means of noncollinear $\vec{k}$ vector matching. A collinear singly resonant oscillator of this type was first demonstrated by Bjorkholm [33], [34], and some of his results are shown in Fig. 15. Spectra of a doubly resonant oscillator are shown in (a), (b), and (c) for increasing pump power. Oscillation occurred in three clusters which had a spacing of about 12 Å. Part (d) shows the spectra of his singly resonant oscillator in which, in all cases, clusters were absent. Other oscillators having only their signal or idler frequencies resonant have been constructed by Falk and Murray [29] and by Belyaev et al. [35]. The oscillator of Falk and Murray was noncollinear and is shown schematically in Fig. 10. Though no clusters were observed, an additional unexplained spectral component was often found a number of angstroms away from the primary component. Belyaev et al. also found a spectrum consisting of one or two lines spaced by a few angstroms; with the width of each individual line not exceeding 0.1 cm^{-1}.

At this time an experimental study of the competition between the longitudinal modes of a single cavity parametric oscillator has not been accomplished. A theoretical study by Kreuzer [36] has shown that if the oscillator is operated less than 4.81 times above threshold, that it should saturate uniformly and in the steady state have only a single oscillating longitudinal mode. For an oscillator operated further above threshold, the steady-state solution may consist of two or more longitudinal modes. For the latter situation, the pump is periodically depleted and restored inside the nonlinear crystal resulting in a saturated lineshape which is broadened and double peaked.

C. Locking

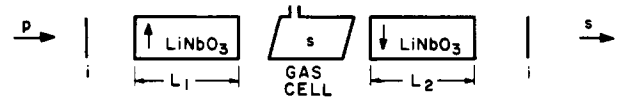Many experiments require an oscillator output with far greater stability than that presently available. For instance,

optical pumping of gaseous vibrational or rotational lines will require frequency control of better than 0.03 cm^{-1}. One proposed approach which may make it possible to lock the output of an optical parametric oscillator onto a gaseous atomic absorption line is shown in Fig. 16 [37]. The usual single nonlinear crystal is replaced by two nonlinear crystals which have the direction of their +z axes reversed. Between the reversed nonlinear crystals is placed the cell containing the gas to which it is desired to lock the output frequency of the oscillator. If the absorbing transition is at the signal frequency of the oscillator, then the oscillator is made resonant at only the idler frequency. As a result of the reversed positive axes, the parametric gain of the first crystal is partially cancelled by the second crystal. That is, the relative phases of the signal, idler, and pump on entering the second crystal are such that instead of further gain the signal and idler decay to the values which they had on entering the first crystal. The pressure of an absorbing gas is then adjusted until it is nearly opaque at the pertinent atomic transition. The loss and phase shift of this gas prevents the gain cancellation in the second crystal, with a resultant sharply peaked gain function centered at the frequency of the atomic transition.

Bjorkholm has shown that it is possible to lock, at least on a transient basis, the output of a high-power pulsed optical parametric oscillator to an incident low level signal. In a recent experiment he succeeded in locking a LiNbO$_3$ oscillator, pumped by a ruby laser, to a stabilized CW YAG laser [38]. A minimum locking power of 1 mW, and a locking range of about 15 Å were obtained.

V. Saturation and Power Output

If the level of the pumping field is above threshold, the signal and idler fields build up and deplete the pump as it passes through the crystal. Saturation occurs when the pump intensity, appropriately averaged over the length of the nonlinear crystal, is reduced to the point where single pass gain equals single pass loss.

We first consider the case where only the signal frequency is resonant and determine the pumping power necessary to attain appreciable conversion efficiency. We assume that the round-trip cavity loss and thus the saturated single pass gain at the signal frequency are sufficiently small so that the signal field may be assumed constant over the length of the nonlinear crystal. It should be noted that this is a small gain as opposed to a small power assumption. Equation (3a) and (3c) may be solved subject to $E_i = 0$, and $E_p = E_p(0)$ at $z = 0$. Taking E_s as an undetermined constant, we find

$$E_i = -j \frac{\eta_i \omega_i d E_s^* E_p(0)}{\beta} \exp - j \frac{\Delta kL}{2} \sin \beta L$$

$$E_p = E_p(0) \exp j \frac{\Delta kL}{2} \left[\cos \beta L - j \frac{\Delta k}{2\beta} \sin \beta L \right], \quad (29)$$

where

$$\beta = \left[\omega_i \omega_p \eta_i \eta_p d^2 |E_s|^2 + \Delta k^2/4 \right]^{1/2}.$$

From (5) the generated signal power is related to the generated idler power, and thus

$$|E_s(L)|^2 - |E_s(0)|^2 = \frac{\omega_s \omega_i \eta_s \eta_i d^2 |E_s|^2 |E_p(0)|^2}{\beta^2} \sin^2 \beta L. \quad (30)$$

The single pass power gain $G = (|E_s(L)|^2 - |E_s(0)|^2)/|E_s(0)|^2$ is now set equal to the round-trip power loss $2\alpha_s$. Thus

$$\omega_s \omega_i \eta_s \eta_i d^2 |E_p(0)|^2 L^2 \frac{\sin^2 \beta L}{\beta^2 L^2} = 2\alpha_s. \quad (31)$$

With the pump level $E_p(0)$ fixed, $|E_s|$ is determined by the solution of (31). At threshold, the $|E_s| = 0$ and therefore $\beta = 0$ ($\Delta k = 0$), yielding a threshold power in agreement with (25). At line center, we see from (29), that the pump will be completely depleted when $\beta L = \pi/2$; from (31), that this will occur at a pumping power equal to $(\pi/2)^2$ times the threshold pumping power [36]. If the value of the pumping field is increased further, the pump will again begin to grow at the expense of the signal and idler field. As noted at the end of the last section, this spatially varying pump field creates an interesting type of line broadening first pointed out by Kreuzer [36].

A parametric oscillator with only its signal frequency resonant has the advantage that if the desired output of the oscillator is taken at the idler frequency, then an optimum coupling problem is avoided. That is, at any drive level the signal cavity should be made as lossless as possible. If the pump is adjusted to $(\pi/2)^2$ times its threshold value, then ω_i/ω_p of the incident pump power will be obtained at the output [33]. In a recent experiment, Falk and Murray [29] have obtained about 70 percent peak power conversion and 50 percent energy conversion from the incident ruby beam. As seen from the power-versus-time plots in Fig. 17, greater energy conversion was prevented by the build-up time of the oscillator. The schematic of this oscillator is shown in Fig. 10.

We next consider the case where both the signal and idler cavities are resonant. Here the signal and idler waves travel through the nonlinear media in both the forward and backward directions. When traveling in the backward direction, they mix to produce a pump wave traveling in the opposite direction from the incident pump wave. As first pointed out by Siegman [39], this results in a power-dependent reflection of the pump and a limiting of the transmitted pump to its threshold value. As a result, the maximum efficiency of such an oscillator is 50 percent and occurs at a pump power equal to four times the threshold pump power.

Bjorkholm has recently shown that if this backward reflection is avoided, the signal and idler resonant case may
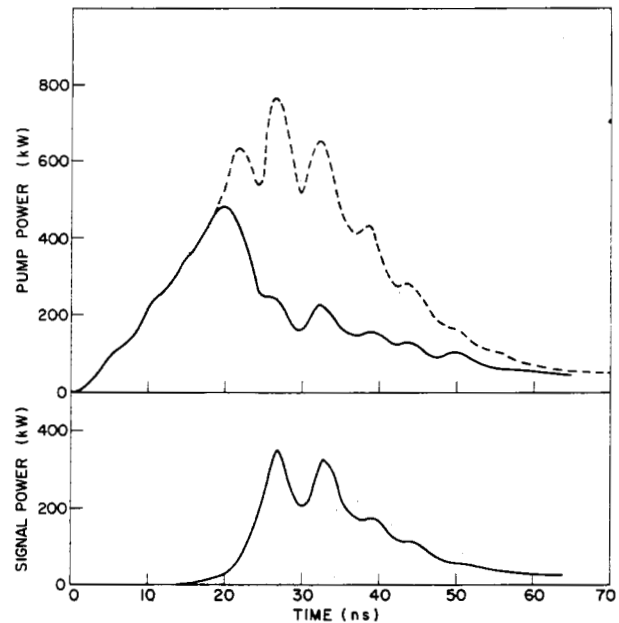

Fig. 17. Output power of noncollinear single cavity oscillator. The dashed curve shows the pump in the absence of the parametric interaction. (From Falk and Murray [29].)

also be 100 percent efficient [40]. With power-dependent pump reflections absent, the generated signal and idler powers are given by

$$\frac{\omega_p}{\omega_s} \frac{P_s}{P_p} = \frac{\omega_p}{\omega_i} \frac{P_i}{P_p} = 4 \frac{P_t}{P_p} \left[(P_p/P_t)^{1/2} - 1 \right], \quad (32)$$

where P_t is the threshold pumping power. At four times above threshold, 100 percent conversion efficiency is obtained. Fig. 18 shows the efficiency and the ratio of transmitted-to-incident pump power for the doubly resonant oscillator with and without power-dependent reflections.

Byer et al. have recently constructed a CW argon pumped ring-cavity parametric oscillator [41], shown in Fig. 19. The oscillator builds up in the direction in which the pumping wave is traveling and power-dependent reflections are avoided. Though 60 percent depletion of the incident pumping beam was observed, as a result of insufficient output coupling only a few milliwatts of output power were obtained.

Ammann et al. have recently obtained about 7 percent average power conversion in a doubly resonant $LiNbO_3$ oscillator directly pumped by a repetitively Q-switched $Nd^{3+}:YAG$ laser [42].

Another interesting type of optical parametric oscillator is obtained when the nonlinear crystal is placed inside the cavity of the pumping laser. The mirrors for the signal and idler cavity may be coincident with those of the pumping laser or may be positioned using various types of beam splitters. Oshman and Harris [43] have shown theoretically that this type of oscillator may operate in several types of regimes. These are: an efficient regime with operating characteristics similar to those of the previously described oscillators; an inefficient regime in which the parametric coupling in effect drives the phase rather than the amplitude
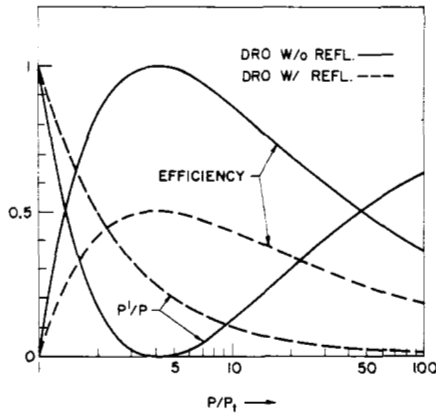
Fig. 18. Efficiency and transmitted pump power of the doubly resonant oscillator, with and without power dependent pump reflection. P'/P is the ratio of transmitted-to-incident pump power. (From Bjorkholm [40].)
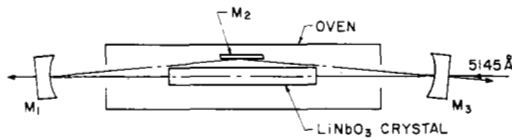

Fig. 19. Ring cavity parametric oscillator where M_1 and M_3 are 5 cm dielectric mirrors, and M_2 is a flat gold mirror. (Byer et al. [41].)

of the oscillation and where a shift of the signal, idler, and pump frequencies from their normal positions is observed; and a repetitively pulsing regime, characterized by short pulses of output power at the signal and idler. A stability analysis of these various regions shows that they are mutually exclusive and can be experimentally chosen by changing the laser gain, the oscillator output coupling, or the strength of the nonlinear interaction.

VI. SPONTANEOUS PARAMETRIC EMISSION

When light from a pumping laser is incident on a nonlinear crystal, there is spontaneous probability that pump photons will split into signal and idler photons. Without the need for optical resonators at either the signal or idler wavelengths, emission at these wavelengths may be observed. This emission has alternately been termed as spontaneous parametric emission, parametric fluorescence, parametric noise, parametric luminescence, and parametric scattering [44]–[49]. It is analogous to laser fluorescence or more exactly to spontaneous Raman and Brillouin scattering. It is important since even at pump fields which are far too low to attain oscillation it may still be observed and used to obtain temperature, angular, or electrooptic tuning curves of potential oscillator materials. The data for Figs. 6 and 8 were obtained using this technique. The fact that the spontaneously emitted power varies linearly with pump power and is independent of both the area and coherence of the pumping beam, also makes it a useful tool for the measurement of optical nonlinearities.

Spontaneous parametric emission was predicted and studied by Louisell et al. [47] and others, and was first observed at optical frequencies by Akhmanov et al. [48], Magde and Mahr [26], and Harris et al. [50].
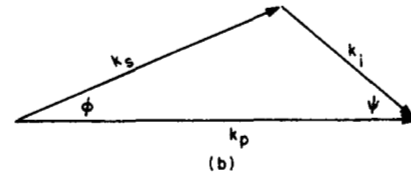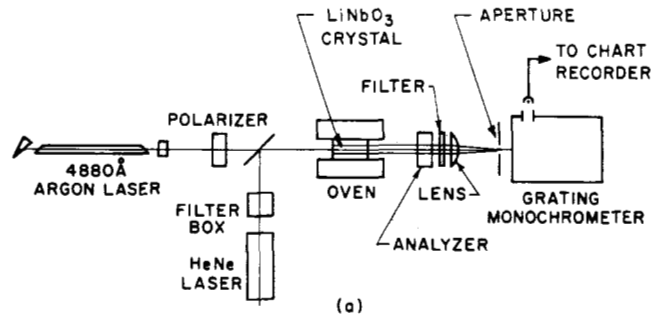

Fig. 20. (a) Apparatus for viewing spontaneous parametric emission. (b) $\vec{k}$ vector matching. (From Byer and Harris [31].)

The transition rate for spontaneous parametric emission may be calculated by forming an interaction Hamiltonian based on the nonlinear susceptibility, and then applying first order perturbation theory. Kleinman [51] and Tang [52] have shown that this approach yields the now-accepted result that the parametric emission may be considered to arise as the result of the mixing of a fictitious zero-point flux, at both the signal and idler frequency, with the incoming pump beam [31]. The effective zero-point flux is obtained by allowing one half-photon to be present in each blackbody mode of a quantizing volume. The result is a generated polarization which attempts to radiate at all frequencies and in all directions. Its ability to radiate effectively is determined by the degree of velocity synchronism with the free wave at the given frequency and in the given direction.

A typical experiment for viewing spontaneous parametric emission is shown in Fig. 20. The pump propagates along the length of a $LiNbO_3$ crystal and is polarized along its optic axis. The signal and idler waves are ordinary waves and make angles ϕ and ψ, respectively, with the pump wave. For a plane wave pump, for small ϕ and ψ, the incremental spontaneously radiated signal power [31] in a bandwidth $d\omega$ and angle $d\phi$ is given by

$$dP_s = \beta L^2 P_p f(\omega_s, \phi)\phi \, d\phi \, d\omega, \tag{33}$$

where

$$B = \frac{2\omega_s^4 \omega_i d_{15}^2 \hbar n_s}{(2\pi)^2 e_0^3 c^5 n_i n_p},$$

and $f(\omega_s, \phi)$ is the velocity synchronism reduction factor given by

$$f(\omega_s, \phi) = \frac{\sin^2(|\Delta k|L/2)}{(|\Delta k|L/2)^2}, \tag{34}$$

where $|\Delta k|$ is the length of the wave vector mismatch taken in the direction of the pump. For small angles and small dispersion Δk may be written
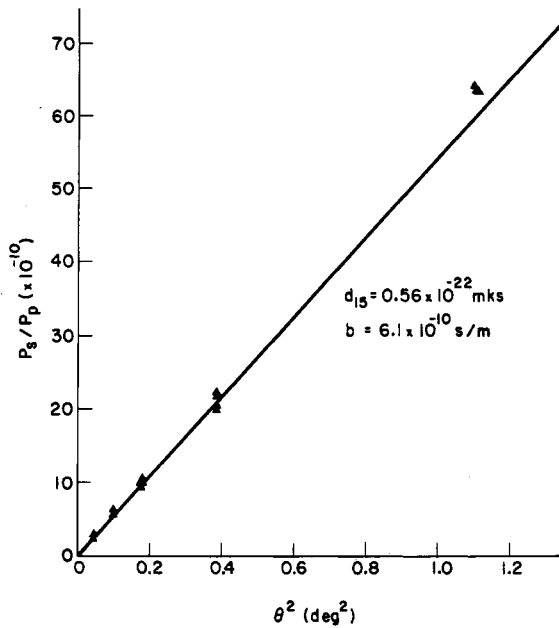
Fig. 21. Total spontaneously emitted power versus θ^2, showing theoretical and experimental results. (From Byer and Harris [31].)
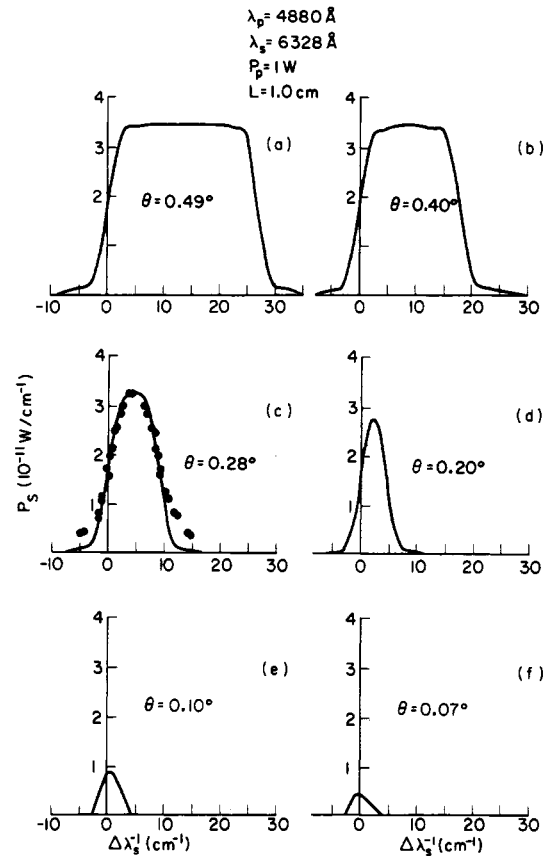

Fig. 22. Spectral distribution of spontaneous power at different acceptance angles. Part (c) shows experimental points normalized to peak of the theoretical curve. (From Byer and Harris [31].)

$$\Delta k = + bd\omega_s + g\phi^2, \tag{35}$$

where

$$g = k_s k_p / 2k_i,$$

and b is defined in (27). As a result of normal dispersion, b is negative, and thus higher frequencies will be obtained farther off angle.

Combining (33), (34), and (35), the total radiated power over all frequencies in a given acceptance angle θ is

$$P_s = \beta L^2 P_p \int_{-\infty}^{+\infty} \int_0^\theta \mathrm{sinc}^2 \left[\tfrac{1}{2}(b\omega_s + g\phi^2)L\right]\phi d\phi\, d\omega_s, \tag{36}$$

which may be integrated [31] to yield

$$P_s = (\beta L P_p/b)\pi\theta^2. \tag{37}$$

The total spontaneously emitted signal power thus varies linearly with the accepted solid angle $\pi\theta^2$, pump power, and crystal length. Noting (33) it is seen to vary as the fourth power of signal frequency and the first power of the idler frequency.

The ratio of the spontaneously emitted power to the incident pumping power as a function of θ^2 is shown in Fig. 21 for a 1.1 cm crystal of LiNbO$_3$ and a CW 4880 Å pump. The triangular points are experimental and the solid line is theoretical.

The spectral distribution of the spontaneously emitted light as a function of the accepted angle θ is shown in Fig. 22. The theoretical curves were obtained by numerically integrating (36). As θ is decreased the bandwidth is at first reduced, but then approaches the limiting bandwidth $(1/bL)$ of a collinear interaction.

A detailed study of spontaneous parametric emission has been given by Kleinman [51]. He makes use of a matching surface, such as is shown in Fig. 23, which is the locus of signal and idler $\bar{k}$ vectors such that $\Delta k = 0$. For the special
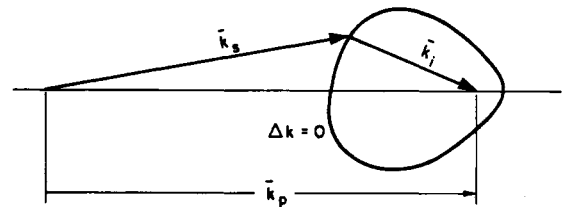

Fig. 23. Kleinman's matching surface [51].

case of emission tangent to this surface both the power and bandwidth of the spontaneously emitted signal are greatly enhanced. This effect can be considered to arise as a result of a greater number of idler modes which may contribute to the emission in the given direction and is analogous to the increased spontaneous emission which occurs when near degeneracy.

Kleinman also discusses a background spontaneous emission which is independent of crystal length and which occurs in directions where phase matching is not possible [51]. This nonphase matched emission is much smaller than the phase matched emission and has thus far not been observed.

Giallorenzi and Tang have observed and discussed spontaneous parametric emission for the case where the idler frequency lies in the infrared absorbing region of the crystal [53], and they find the intensity to be approximately the same as it would have been had there been no absorp-
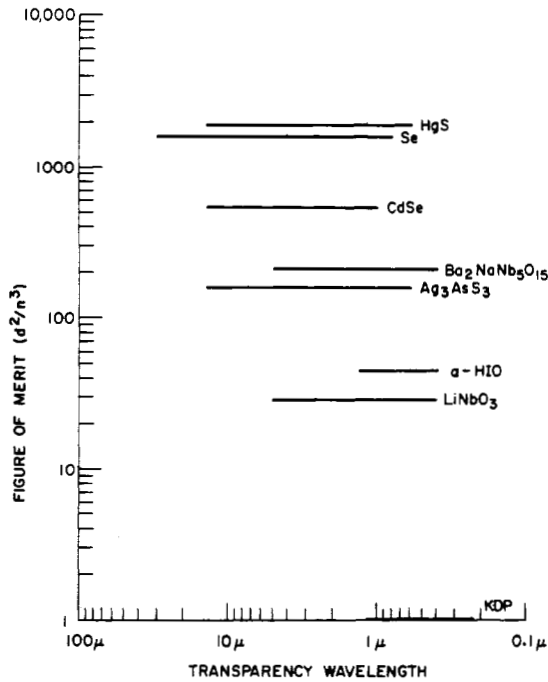
Fig. 24. d^2/n^3 and transparency of some phase matchable nonlinear optical materials.

Fig. 25. Second harmonic generation versus temperature for good and bad crystals of LiNbO₃. A high quality crystal should have a half-power width of about 0.64° C/L where L is its length in centimeters.

tion. With one frequency in the absorbing region, spontaneous emission provides a convenient means to obtain the dispersion curve in the lossy region.

Recently four-photon parametric noise, corresponding to satisfaction of frequency and $\bar{k}$ vector conditions of the form $\omega_p + \omega_p = \omega_s + \omega_i$ and $\bar{k}_p + \bar{k}_p = \bar{k}_s + \bar{k}_i$, has been observed in water by Weinberg [54] and in calcite by Meadors et al. [55]. The potential advantage of a four-frequency process of this type is that the pump may be a lower frequency than the signal. Using a ruby pump, Meadors et al. tuned from 4300 Å to 5900 Å. For a four-photon process of this type, unlike the three-photon process, focusing of the pump is of consequence.

If the parametric gain is sufficient, spontaneous emission may be directly amplified without using optical resonators. One technique, demonstrated by Akmanov et al. [56] uses multiple reflections between roof top prisms. With a pump density of 70 MW/cm² of doubled 1.06 μ light, 100 kW of tunable radiation was obtained. The nonlinear crystal used was ADP, and tuning was accomplished by crystal rotation. Observed linewidths were about 1–2 Å.

VII. NONLINEAR OPTICAL MATERIALS

From the considerations of the previous sections, a number of desirable qualities for materials to be used in optical parametric oscillators may be formulated. These are: high nonlinearity; phase matchability and, in particular, 90° phase matchability; narrow linewidth (large b); high transparency and freedom from damage; and large variation of refractive indices with temperature, angle, pressure, or electric field. Fig. 24 shows d^2/n^3 (see Section II) and the transparency range of a number of phase matchable materials. Normalization is to d^2/n^3 for KDP. Since both d and n are dependent on the particular angle and frequencies at
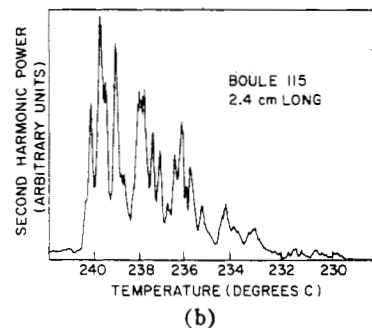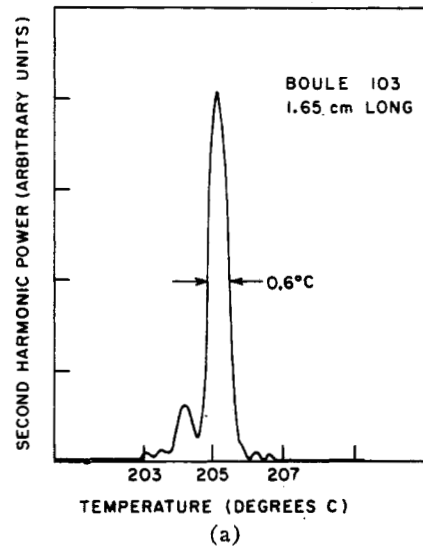
which phase matching occurs, there is some uncertainty to the values in this figure.

The KDP-ADP type materials are the only ones with UV transparency [57]–[59] and, as seen in Figs. 6 and 8, allow convenient visible tunability. These crystals might also be used to double a tunable visible source into the 2700 Å–3000 Å region [57]. Unfortunately, Dowley has found that these crystals exhibit some form of UV damage which limits the average power which may be obtained when doubling the 5145 Å line of argon [58]. KDP-ADP type materials have been found to withstand very high optical power densities (>400 MW/cm²) before exhibiting surface damage [60] and are particularly useful for high power Q-switched applications. When operated near their Curie temperature these materials should also allow wide electrooptic tuning [61].

LiNbO₃ has a very useful visible and IR transparency range, and is the most widely used oscillator material at this time [62]–[65]. Crystals of excellent optical quality are now available in 4 to 5 cm lengths. Great care must be taken to grow this material such that its refractive index does not vary with distance in the crystal [66], [67] $\bar{k}$ vector matching for a 4 cm crystal requires that the variation of refractive indices be less than 10^{-5}. It has been found that this is best achieved by growing from a melt which is about 2 percent lithium deficient. Fig. 25 shows second harmonic power versus temperature for a high quality and a low quality LiNbO₃ crystal. For the poor crystal, the refractive

index varies with distance, and different parts of the crystal phase match at different temperatures. For second harmonic generation from 1.15 μ, the half-power width for a high quality crystal should be about 0.64°C/L, where L is the length in centimeters of the nonlinear crystal. As a result of optical refractive index damage, $LiNbO_3$ must be maintained at a temperature greater than about 170°C when in the presence of intense visible radiation [68]. In a repetitively pulsed system surface damage probably occurs somewhere in the vicinity of 20 MW/cm².

$Ba_2NaNb_5O_{15}$ has a similar transparency range as $LiNbO_3$ and a d^2/n^3 which is almost ten times greater [69]–[71]. However, available crystals have lengths of 4 mm or less, and typically exhibit severe striations. At room temperature the material does not exhibit refractive index damage, but on the other hand its phase transition at about 300°, and the decrease of its nonlinearity above this transition, limit its temperature tuning range.

Two possible crystals for oscillation further in the infrared are proustite (Ag_3AsS_3) and CdSe [72]–[74]. Though proustite has been used for mixing experiments, an oscillator using it has not yet been constructed. As a result of its large birefringence, only off angle $\bar{k}$ vector matching will be possible. Also, the material is reported to damage relatively easily, i.e., at about 1 MW/cm². An absorption band with absorption of about 1 cm⁻¹ at 10.6 μ will probably prevent working with the CO_2 laser.

CdSe has a high nonlinearity [74] and should be phase matchable near 90° for a pump at about 2.5 μ.

Tellurium had attracted earlier interest when Patel used it both for doubling CO_2 [75] and to obtain a parametric gain of 3 dB at 18 μ [76]. d^2/n^3 is about 1.7 10⁶ on the normalized scale of Fig. 21. However, the material is hard to handle and has a relatively high loss.

Some other possible nonlinear crystals for use in oscillator applications are discussed in [77]–[84].

The conventions for specifying optical nonlinearity have caused some confusion, and may be summarized as follows [13]. If the electric field and polarization waves are written in the form

$$E_i(t) = \text{Re}\left[E_i(\omega)\exp j\omega t\right]$$

and

$$\mathscr{P}_i(t) = \text{Re}\left[\mathscr{P}_i(w)\exp j\omega t\right], \tag{38}$$

then for three interacting frequencies with $\omega_3 = \omega_1 + \omega_2$, the generated polarization is given by

$$\mathscr{P}_i(w_3) = \sum_j\sum_k \chi_{ijk}(-\omega_3,\omega_1,\omega_2)E_j(\omega_1)E_k(\omega_2)$$

$$\mathscr{P}_i(w_2) = \sum_j\sum_k \chi_{ijk}(-\omega_2,-\omega_1,\omega_3)E_j^*(\omega_1)E_k(\omega_3) \tag{39}$$

$$\mathscr{P}_i(w_1) = \sum_j\sum_k \chi_{ijk}(-\omega_1,-\omega_2,\omega_3)E_j^*(\omega_2)E_k(\omega_3).$$

The nonlinear susceptibility coefficients χ_{ijk} satisfy what is termed as overall permutation symmetry, which states that the subscripts and frequencies may be permuted in any order. For instance

$$\chi_{ijk}(-\omega_3,\omega_1,\omega_2) = \chi_{jik}(\omega_1,-\omega_3,\omega_2)$$
$$= \chi_{kji}(\omega_2,\omega_1,-\omega_3). \tag{40}$$

Overall permutation symmetry in effect states that if three frequencies are involved in a lossless nonlinear process, that irrespective of which is doing the generating, or being generated, the nonlinear coefficient governing the process is the same.

The above χ_{ijk} are related to the d_{ijk} which are used to describe second harmonic generation by

$$\chi_{ijk}(-2\omega,\omega,\omega) = 2d_{ijk}(-2\omega,\omega,\omega). \tag{41}$$

Since d_{ijk} is symmetric in the subscripts j and k, it is expressed in the usual abbreviated notation where $d_{ijk} = d_{il}$ according to $l = 1, 2, 3, 4, 5, 6$ for $jk = 11, 22, 33, 23, 13, 12$, respectively. For lossless media these coefficients may be shown to be real, and their small dispersion over the transparency range of the crystal is usually neglected. In cases where the direction of optical propagation is not along the principal crystal axes, it is necessary to take the projection of the generated polarizations in the directions of the respective optical $\bar{E}$ fields. The resulting coefficients have been termed as effective nonlinear coefficients, and their value for a number of uniaxial crystal classes have been tabulated by Boyd and Kleinman [13].

VIII. TUNABLE FAR-INFRARED GENERATION

There is great interest in extending tunable source techniques to the far IR region of the spectrum, where relatively conventional sources are at their poorest. Assuming other factors constant, the pump power necessary to achieve a given gain increases inversely as the square of the lower frequency. Also, in the far IR losses are typically somewhat greater than in the visible or near IR, and thus significantly larger nonlinearities are required. Such nonlinearities may be obtained either by making use of a very high index material, such as tellurium, or by operating with the IR frequency below the Reststrahl frequencies, and thus gaining the contribution of the lattice to the nonlinear coefficient. For instance, in $LiNbO_3$, the nonlinear coefficient governing the interaction between a microwave frequency and two optical frequencies is approximately 30 times greater than the nonlinear coefficient relating three similarly polarized optical frequencies. (This may be deduced by converting the light modulation coefficient r_{51} into an equivalent d coefficient.) Two other principal changes may occur when one of the interacting frequencies lies below the lattice absorption frequencies. First, the lattice contribution to the low-frequency dielectric constant often creates the situation where the sum of the signal and idler $\bar{k}$ vectors is greater than the pump $\bar{k}$ vector. This allows noncollinear phase matching of three waves of the same polarization. (By contrast, as a result of normal dispersion, at optical frequencies $|k_s| + |k_i| < |k_p|$.) Second, it is usually necessary to include the effect of loss on the low-frequency wave.

As the IR frequency approaches one of the vibrational modes of the lattice an increasing fraction of its energy is
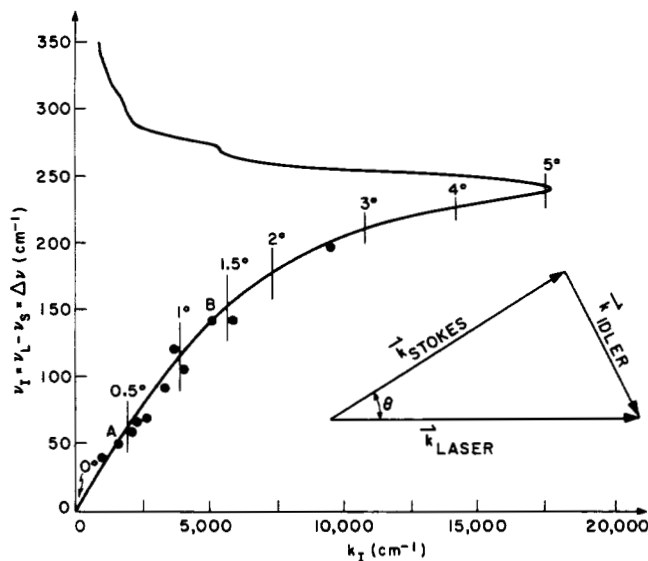
Fig. 26. Dispersion of the A_1 symmetry 248 cm^{-1} polariton mode of LiNbO$_3$. The vertical lines intersecting the dispersion curve denote the value of θ necessary for $\bar{k}$ vector matching. (From Yarborough et al. [89].)

Fig. 27. Parametric gain, absorption coefficient, and ratio of IR to Stokes power, as a function of frequency near the 366 cm^{-1} lattice resonance of gallium phosphide. (a) Relative parametric gain. (b) IR absorption coefficient. (c) Ratio of IR to Stokes power densities (S_1/S_2). The solid portion of the curve denotes the region over which phase matching is possible. (From Henry and Garrett [90].)

mechanical rather than electromagnetic, and in this region it is often termed a polariton mode [85]. Gain results from the interaction with both the vibrational and electromagnetic portions of the mode; and to the extent that the vibrational portion is important, it may be considered as a tunable Raman gain [86], [87].

In two recent experiments, Gelbwachs et al. [88] and Yarborough et al. [89] have obtained tunable radiation in the vicinity of the A_1 symmetry 248 cm^{-1} polariton mode of LiNbO$_3$. The dispersion diagram for this mode is shown in Fig. 26. The vertical lines intersecting the dispersion curve denote the value of the angle θ between the pump and the Stokes beams which is necessary for $\bar{k}$ vector matching. (In analogy with the usual Raman process, the upper frequency is termed as the Stokes wave). As θ is varied, the oscillator is tuned. In the Gelbwachs et al. experiment [88], tuning was accomplished by varying the angle between the laser beam and the axis of a high-Q resonator. In the Yarborough et al. experiment [89], opposite faces of the crystal were polished flat and parallel and an external resonator was not employed. Infrared tuning from 50 μ to 238 μ was obtained with a conversion efficiency to the Stokes frequency of greater than 50 percent. Though infrared powers were not measured, it was estimated that about 70 watts were generated inside the crystal at $\lambda \cong 50 \mu$.

As the infrared frequency approaches the lattice resonance, both the absorption coefficient and the nonlinear susceptibility become resonately large, though in such a manner as to leave the gain relatively unchanged. Fig. 27 shows theoretical results of Henry and Garrett [90] as the infrared frequency is swept through the 366 cm^{-1} lattice resonance of gallium phosphide. The absorption coefficient, parametric gain, and the ratio of generated infrared to Stokes radiation are shown. The solid portion of the curves indicate the region over which phase matching is possible.
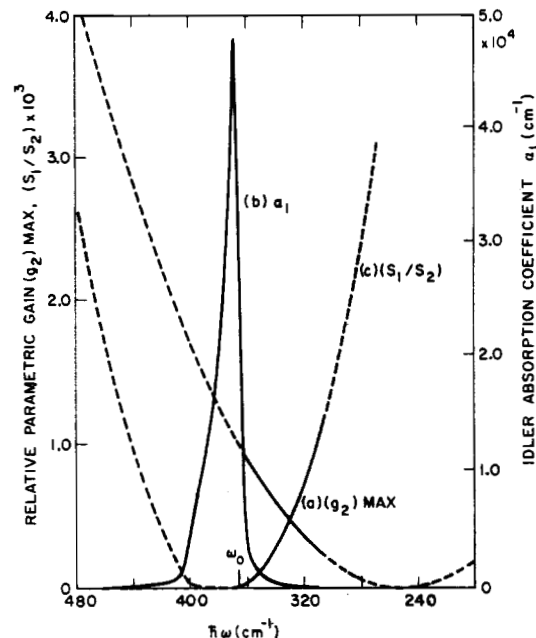
The slow variation of the gain coefficient and its approach to zero at about 250 cm^{-1} is a result of destructive interference between the parametric and Raman type portions of the gain coefficient. This interference has been verified experimentally by Faust and Henry [91].

Though the resonant behavior of the infrared absorption does not substantially affect the gain, it may greatly influence the production of infrared radiation. Henry and Garrett [90] have shown that the ratio of infrared to Stokes powers is approximately

$$P_{\text{IR}}/P_{\text{Stokes}} = \frac{\omega_i}{\omega_s} \frac{G}{\alpha_{\text{IR}}},$$

where G is the gain and α_{IR} is the infrared loss coefficient. As seen in Fig. 27, though in the vicinity of the resonance the gain is relatively unaffected, the IR power drops sharply.

Far-infrared radiation has also been obtained by difference frequency mixing of higher frequencies. Van Tran and Patel [92] have recently reported the use of a magnetic field to achieve phase matched difference frequency generation in InSb. Phase matching was accomplished by varying the cyclotron frequency and thus the free carrier contribution to the refractive index. Discrete tuning from 95 μ to 105 μ was obtained by mixing a number of wavelengths of two synchronously Q-switched CO$_2$ lasers. Previously, nonphase matched far-infrared generation has been reported by Zernike [93].

Two other approaches to tunable generation in the far infrared are backward wave oscillation in a material with low birefringence such as LiTaO$_3$ [94], [95], and Raman down shifting of higher frequency tunable radiation.

REFERENCES

[1] P. A. Franken, A. E. Hill, C. W. Peters, and G. Weinreich, "Generation of optical harmonics," *Phys. Rev. Letters*, vol. 7, p. 118, August 1961.

[2] R. H. Kingston, "Parametric amplification and oscillation at optical frequencies," *Proc. IRE* (Correspondence), vol. 50, p. 472, April 1962.

[3] N. M. Kroll, "Parametric amplification in spatially extended media and application to the design of tunable oscillators at optical frequencies," *Phys. Rev.*, vol. 127, p. 1207, August 1962.

[4] S. A. Akhmanov and R. V. Khokhlov, "Concerning one possibility of amplification of light waves," *J. Exptl. Theoret. Phys.*, vol. 16, p. 252, January 1963.

[5] J. A. Armstrong, N. Bloembergen, J. Ducuing, and P.S. Pershan, "Interactions between light waves in a nonlinear dielectric," *Phys. Rev.*, vol. 127, p. 1918, September 1962.

[6] C. C. Wang and C. W. Racette, "Measurement of parametric gain accompanying optical difference frequency generation," *Appl. Phys. Letters*, vol. 6, p. 169, April 1965.

[7] J. A. Giordmaine and R. C. Miller, "Tunable coherent parametric oscillation in LiNbO$_3$ at optical frequencies," *Phys. Rev. Letters*, vol. 14, p. 973, June 1965.

[8] W. H. Louisell, *Coupled Mode and Parametric Electronics*. New York: Wiley, 1960.

[9] R. W. Minck, R. W. Terhune, and C. C. Wang, "Nonlinear optics," *Appl. Opt.*, vol. 5, p. 1595, October 1966.

[10] N. Bloembergen, *Nonlinear Optics*. New York: W. A. Benjamin, Inc., 1965, p. 135.

[11] J. A. Giordmaine and R. C. Miller, "Optical parametric oscillation in LiNbO$_3$," in *Physics of Quantum Electronics*, P. L. Kelley, B. Lax, and P. E. Tannenwald, Eds. New York: McGraw-Hill, 1966, pp. 31–42; also available in *Proc. Physics of Quantum Electronics Conf.* (San Juan, Puerto Rico), June 28–30, 1965.

[12] J. A. Giordmaine, "Parametric Optics," Academic Press, to be published; and presented in Quantum Optics Course XVIII, Internatl. School of Physics, Varenna, July 19–August 21, 1967.

[13] G. D. Boyd and D. A. Kleinman, "Parametric interaction of focused Gaussian light beams," *J. Appl. Phys.*, vol. 39, p. 3597, July 1968.

[14] G. D. Boyd and A. Ashkin, "Theory of parametric oscillator threshold with single-mode optical masers and observation of amplification in LiNbO$_3$," *Phys. Rev.*, vol. 146, p. 187, June 1966.

[15] R. G. Smith, J. E. Geusic, H. J. Levinstein, J. J. Rubin, S. Singh, and L. G. Van Uitert, "Continuous optical parametric oscillation in Ba$_2$NaNb$_5$O$_{15}$," *Appl. Phys. Letters*, vol. 12, p. 308, May 1968.

[16] R. G. Smith, "Nonlinear optics: recent advances," Invited paper, presented at the 1969 Conf. Laser Engrg. and Appl., Washington, D. C., May 1969.

[17] S. E. Harris, "Threshold of multimode parametric oscillators," *IEEE J. Quantum Electronics*, vol. QE-2, pp. 701–702, October 1966.

[18] H. Hsu, "Parametric interactions involving multiple elementary scattering processes," *J. Appl. Phys.*, vol. 38, p. 1787, March 1967.

[19] R. L. Byer, M. K. Oshman, J. F. Young, and S. E. Harris, "Visible CW parametric oscillator," *Appl. Phys. Letters*, vol. 13, p. 109, August 1968.

[20] S. E. Harris, "Threshold of phase-locked parametric oscillators," *IEEE J. Quantum Electronics*, vol. QE-3, pp. 205–206, May 1967.

[21] M. V. Hobden and J. Warner, "The temperature dependence of the refractive indices of pure lithium niobate," *Phys. Letters*, vol. 22, p. 243, August 1966.

[22] J. G. Bergman, A. Ashkin, A. A. Ballman, J. M. Dziedzic, H. J. Levinstein, and R. G. Smith, "Curie temperature, birefringence, and phase-matching temperature variations in LiNbO$_3$ as a function of melt stoichiometry," *Appl. Phys. Letters*, vol. 12, p. 92, February 1968.

[23] J. A. Giordmaine and R. C. Miller, "Optical parametric oscillation in the visible spectrum," *Appl. Phys. Letters*, vol. 9, p. 298, October 1966.

[24] M. W. Dowley, private communication.

[25] R. C. Miller and W. A. Nordland, "Tunable LiNbO$_3$ optical parametric oscillator with external mirrors," *Appl. Phys. Letters*, vol. 10, p. 53, January 1967.

[26] D. Magde and H. Mahr, "Study of ammonium dihydrogen phosphate of spontaneous parametric interaction tunable from 4400 to 16000 Å," *Phys. Rev. Letters*, vol. 18, p. 905, May 1967.

[27] L. B. Kreuzer, "Ruby-laser-pumped optical parametric oscillator with electro-optic effect tuning," *Appl. Phys. Letters*, vol. 10, p. 336, June 1967.

[28] G. V. Krivoshchekov, S. V. Kruglov, S. I. Marennikov, and Y. N. Polivanov. "Variation of the emission wavelength of a parametric light generator by means of an external electric field," *Zh. Eksperim. i Teor. Fiz.*, vol. 7, p. 84, February 1968.

[29] J. Falk and J. E. Murray, "Single cavity noncollinear parametric oscillation," *Appl. Phys. Letters*, vol. 14, p. 245, April 1969.

[30] S. A. Akhmanov, A. G. Ershov, V. V. Fadeev, R. V. Khokhlov, O. N. Chunaev, and E. M. Shvom, "Observation of two-dimensional parametric interaction of light waves," *J. Exptl. Theoret. Phys. Letters*, vol. 2, p. 285, November 1965.

[31] R. L. Byer and S. E. Harris, "Power and bandwidth of spontaneous parametric emission," *Phys. Rev.*, vol. 168, p. 1064, April 1968.

[32] A. I. Kovrigin and R. L. Byer, "Stability factor for optical parametric oscillators," *IEEE J. Quantum Electronics*, to be published.

[33] J. E. Bjorkholm, "Efficient optical parametric oscillation using doubly and singly resonant cavities," *Appl. Phys. Letters*, vol. 13, p. 53, July 1968.

[34] ——, "Some spectral properties of doubly and singly resonant optical parametric oscillators," *Appl. Phys. Letters*, vol. 13, p. 399, December 1968.

[35] Y. N. Belyaev, A. M. Kiselev, and J. R. Freidman, "Investigation of parametric generator with feedback in only one of the waves," *J. Expt. Theoret. Phys. Letters*, vol. 9, p. 263, April 1969.

[36] L. B. Kreuzer, "Theory of the singly resonant optical parametric oscillator," to be published.

[37] S. E. Harris, "Method to lock an optical parametric oscillator to an atomic transition," *Appl. Phys. Letters*, vol. 14, p. 335, June 1969.

[38] J. E. Bjorkholm and H. G. Danielmeyer, "Frequency control of a pulsed optical parametric oscillator by radiation injection," presented at the 1969 Conf. Laser Engrg. and Appl., Washington, D. C., May 1969.

[39] A. E. Siegman, "Nonlinear optical effects: an optical power limiter," *Appl. Optics*, vol. 1, p. 739, November 1962.

[40] J. E. Bjorkholm, "Analysis of the doubly resonant optical parametric oscillator without power dependent reflections," *IEEE J. Quantum Electronics*, vol. QE-5, pp. 293–295, June 1969.

[41] R. L. Byer, A. Kovrigin, and J. F. Young, "A CW ring cavity parametric oscillator," Post-deadline paper, 1969 Conf. Laser Engrg. and Appl., Washington, D. C., May 1969.

[42] E. O. Ammann, J. D. Foster, M. K. Oshman, and J. M. Yarborough, "Repetively pumped parametric oscillator at 2.13 μ," presented at the 1969 Conf. Laser Engrg. and Appl., Washington, D. C., May 1969.

[43] M. K. Oshman and S. E. Harris, "Theory of optical parametric oscillation internal to the laser cavity," *IEEE J. Quantum Electronics*, vol. QE-4, pp. 491–502, August 1968.

[44] D. N. Klyshko, "Coherent photon decay in a nonlinear medium," *Zh. Eksperim. i Teor. Fiz.*, vol. 6, p. 490, July 1967.

[45] R. G. Smith, J. G. Skinner, J. E. Geusic, and W. G. Nilsen, "Observations of noncollinear phase matching in optical parametric noise emission," *Appl. Phys. Letters*, vol. 12, p. 97, February 1968.

[46] D. Magde and H. Mahr, "Optical parametric scattering in ammonium dihydrogen phosphate," *Phys. Rev.*, vol. 171, p. 393, July 1968.

[47] W. H. Louisell, A. Yariv, and A. E. Siegman, "Quantum fluctuations and noise in parametric processes. I.," *Phys. Rev.*, vol. 124, p. 1646, December 1961.

[48] S. A. Akhmanov, V. V. Fadeev, R. V. Khokhlov, and O. N. Chunaev, "Quantum noise in parametric light amplifiers," *J. Exptl. Theoret. Phys. Letters*, vol. 6, p. 85, August 1967.

[49] J. Budin, B. Godard, and J. Ducuing. "Noncollinear interactions in parametric luminescence," *IEEE J. Quantum Electronics*, vol. QE-4, pp. 831–837, November 1968.

[50] S. E. Harris, M. K. Oshman, and R. L. Byer, "Observation of tunable optical parametric fluorescence," *Phys. Rev. Letters*, vol. 18, p. 732, May 1967.

[51] D. A. Kleinman, "Theory of optical parametric noise," *Phys. Rev.*, vol. 174, p. 1027, October 1968.

[52] T. G. Giallorenzi and C. L. Tang, "Quantum theory of spontaneous parametric scattering of intense light," *Phys. Rev.*, vol. 166, p. 225, February 1968.

[53] ——, "CW parametric scattering in ADP with strong absorption in the idler band," *Appl. Phys. Letters*, vol. 12, p. 376, June 1968.

[54] D. L. Weinberg, "Four-photon optical parametric noise in water," *Appl. Phys. Letters*, vol. 14, p. 32, 1969.

[55] J. G. Meadors, W. T. Kavage, and E. K. Damon, "Observation of tunable four-photon parametric noise in calcite," *Appl. Phys. Letters*, vol. 14, p. 360, June 1969.

[56] A. G. Akmanov, S. A. Akhmanov, R. V. Kokhlov, A. I. Kovrigin, A. S. Piskarskas, and A. P. Sukhorukov, "Parametric interactions in optics and tunable light oscillators," *IEEE J. Quantum Electronics*, vol. QE-4, pp. 828–837, November 1968.

[57] M. W. Dowley, "Efficient CW second harmonic generation to 2573 Å," *Appl. Phys. Letters*, vol. 13, p. 395, December 1968.

[58] M. W. Dowley and E. B. Hodges, "Studies of high-power CW and quasi-CW parametric UV generation by ADP and KDP in an argon-ion laser cavity," *IEEE J. Quantum Electronics*, vol. QE-4, pp. 552–558, October 1968.

[59] W. J. Deshotels, "Ultraviolet transmission of dihydrogen arsenate and phosphate crystals," *J. Opt. Soc. Am.*, vol. 50, p. 865, September 1960.

[60] W. F. Hagen and P. C. Magnante, "Efficient second-harmonic generation with diffraction-limited and high-spectral-radiance Nd-glass lasers," *J. Appl. Phys.*, vol. 40, p. 2191, January 1969.

[61] N. I. Adams, III and J. J. Barrett, "Electric field control of 90° phasematching in KDP," *IEEE J. Quantum Electronics*, vol. QE-2, pp. 430–435, September 1966.

[62] G. D. Boyd, Robert C. Miller, K. Nassau, W. L. Bond, and A. Savage, "LiNbO₃: an efficient phase-matchable nonlinear optical material," *Phys. Letters*, vol. 5, p. 234, December 1964.

[63] R. C. Miller, G. D. Boyd, and A. Savage, "Nonlinear optical interactions in LiNbO₃ without double refraction," *Appl. Phys. Letters*, vol. 6, p. 77, February 1965.

[64] J. E. Bjorkholm, "Relative signs of the optical nonlinear coefficients d_{31} and d_{22} in LiNbO₃," *Appl. Phys. Letters*, vol. 13, p. 36, July 1968.

[65] ——, "Relative measurement of the optical nonlinearities of KDP, ADP, LiNbO₃ and α-HIO₃," *IEEE J. Quantum Electronics* (Correspondence), vol. QE-4, pp. 970–972, November 1968; see also correction, *IEEE J. Quantum Electronics*, vol. QE-5, p. 260, May 1969.

[66] J. E. Midwinter and J. Warner, "Up-conversion of near infrared to visible radiation in lithium-meta-niobate," *J. Appl. Phys.*, vol. 38, p. 519, February 1967.

[67] R. L. Byer and J. F. Young, "Quality testing of LiNbO₃ crystals," to be published.

[68] A. Ashkin, G. D. Boyd, J. M. Dziedzic, R. G. Smith, A. A. Ballman, J. J. Levinstein, and K. Nassau, "Optically induced refractive index inhomogeneities in LiNbO₃ and LiTaO₃," *Appl. Phys. Letters*, vol. 9, p. 72, July 1966.

[69] J. E. Geusic, H. J. Levinstein, J. J. Rubin, S. Singh, and L. G. Van Uitert. "The nonlinear optical properties of Ba₂NaNb₅O₁₅," *Appl. Phys. Letters*, vol. 11, p. 269, November 1967.

[70] R. G. Smith, J. E. Geusic, H. J. Levinstein, S. Singh, and L. G. Van Uitert, "Low threshold optical parametric oscillator using Ba₂NaNb₅O₁₅," *J. Appl. Phys.*, vol. 39, p. 4030, July 1968.

[71] R. L. Byer, S. E. Harris, D. J. Kuizenga, J. F. Young, and R. S. Feigelson, "Nonlinear optical properties of Ba₂NaNb₅O₁₅ in the tetragonal phase," *J. Appl. Phys.*, vol. 40, p. 444, January 1969.

[72] W. Bardsley, P. H. Davies, M. V. Hobden, K. F. Hulme, O. Jones, W. Pomeroy, and J. Warner, "Synthetic proustite (Ag₃AsS₃): a summary of its properties and uses," *Opto-Electronics*, vol. 1, p. 29, 1969.

[73] K. F. Hulme, O. Jones, P. H. Davies, and M. V. Hobden, "Synthetic proustite (Ag₃AsS₃): a new crystal for optical mixing," *Appl. Phys. Letters*, vol. 10, p. 133, February 1967.

[74] C. K. N. Patel, "Optical harmonic generation in the infrared using a CO₂ laser," *Phys. Rev. Letters*, vol. 16, p. 613, April 1966.

[75] ——, "Efficient phase-matched harmonic generation in tellurium with a CO₂ laser at 10.6 μ," *Phys. Rev. Letters*, vol. 15, p. 1027, December 1965.

[76] ——. "Parametric amplification in the far infrared," *Appl. Phys. Letters*. vol. 9, p. 332, November 1966.

[77] S. K. Kurtz and T. T. Perry. "A powder technique for the evaluation of nonlinear optical materials," *J. Appl. Phys.*, vol. 39, p. 3798, July 1968.

[78] F. N. H. Robinson. "Nonlinear optical coefficients," *Bell Sys. Tech. J.*, vol. 46, p. 913, May–June 1967.

[79] G. Nath and S. Haussühl, "Large nonlinear optical coefficient in phase matched second harmonic generation in LiIO₃," *Appl. Phys. Letters*, vol. 14, p. 154, March 1969.

[80] ——, "Strong second harmonic generation of a ruby laser in lithium iodate," *Phys. Letters*, vol. 29, p. 91, April 1969.

[81] S. K. Kurtz, T. T. Perry, and J. G. Bergman, Jr., "Alpha-iodic acid: solution-grown crystal for nonlinear optical studies and applications," *Appl. Phys. Letters*, vol. 12, p. 186, March 1968.

[82] C. K. N. Patel, R. E. Slusher, and P. A. Fleury, "Optical nonlinearities due to mobile carriers in semiconductors," *Phys. Rev. Letters*, vol. 17, p. 1011, November 1966.

[83] G. D. Boyd, T. H. Bridges, and E. G. Burkhardt, "Up-conversion of 10.6 μ radiation to the visible and second harmonic generation in HgS," *IEEE J. Quantum Electronics*, vol. QE-4, pp. 515–519, September 1968.

[84] F. R. Nash, J. G. Bergman, G. D. Boyd, and E. H. Turner, "Lithium iodate (LiIO₃)—a new nonlinear material," to be published.

[85] C. H. Henry and J. J. Hopfield, "Raman scattering by polaritons," *Phys. Rev. Letters*, vol. 15, p. 964, December 1965.

[86] I. P. Kaminow and W. D. Johnston, Jr., "Quantitative determination of sources of the electro-optic effect in LiNbO₃ and LiTaO₃," *Phys. Rev.*, vol. 160, p. 519, August 1967.

[87] W. D. Johnston, Jr., I. P. Kaminow, and J. G. Bergman, Jr., "Stimulated Raman gain coefficients for LiNbO₃, Ba₂NaNb₅O₁₅, and other materials," *Appl. Phys. Letters*, vol. 13, p. 190, September 1968.

[88] J. Gelbwachs, R. H. Pantell, H. E. Puthoff, and J. M. Yarborough, "A tunable stimulated Raman oscillator," *Appl. Phys. Letters*, vol. 14, p. 258, May 1969.

[89] J. M. Yarborough, S. S. Sussman, H. E. Puthoff, R. H. Pantell, and B. C. Johnson, "Efficient, tunable optical emission from LiNbO₃ without a resonator," *Appl. Phys. Letters*, vol. 15, p. 102, August 1969.

[90] C. H. Henry and C. G. B. Garrett, "Theory of parametric gain near a lattice resonance," *Phys. Rev.*, vol. 171, p. 1058, July 1968.

[91] W. L. Faust and C. H. Henry, "Mixing of visible and near-resonance infrared light in GaP," *Phys. Rev. Letters*, vol. 17, p. 1265, December 1966.

[92] N. Van Tran and C. K. N. Patel, "Free-carrier magneto-optical effects in far-infrared difference-frequency generation in semiconductors," *Phys. Rev. Letters*, vol. 22, p. 463, March 1969.

[93] F. Zernike, Jr. and P. R. Berman, "Generation of far-infrared as a difference frequency," *Phys. Rev. Letters*, vol. 15, p. 999, December 1965.

[94] S. E. Harris, "Proposed backward wave oscillation in the infrared," *Appl. Phys. Letters*, vol. 9, p. 114, August 1966.

[95] John G. Meadors, "Steady-state theory of backward traveling wave parametric interactions," *J. Appl. Phys.*, vol. 40, p. 2510, May 1969.

[96] R. L. Byer, "Parametric fluorescence and optical parametric oscillation," Ph.D. dissertation, Microwave Lab. Rept. 1711, Stanford University, Stanford, Calif., December 1968.

[97] S. A. Akhmanov, A. I. Kovrigin, V. A. Kolosov, A. S. Piskarskas, V. V. Fadeev, and R. V. Khokhlov, "Tunable parametric light generator with KDP crystal," *J. Exptl. Theoret. Phys. Letters*, vol. 3, p. 241, May 1966.

[98] S. A. Akhmanov, O. N. Chunaev, V. V. Fadeev, R. V. Khokhlov, D. N. Klyshko, A. I. Kovrigin, and A. S. Piskarskas, "Parametric generators of light," presented at the 1967 Symp. Mod. Optics, Polytechnic Institute of Brooklyn, Brooklyn, N. Y., March 1967.